

1
2
3
4
5
6
7
8
9
10
11
12
13
14
15
16
17
18
19
20
21
22
23
24
25
26
27
28
29
30
31
32
33
34
35
36
37
38
39
40
41
42
43
44
45
46
47
48
49
50
51
52
53
54
55
56
57
58
59
60

1 **Organosulfate Formation from 2-Methyl-3-Buten-2-ol (MBO) as a Secondary**
2 **Organic Aerosol (SOA) Tracer in the Atmosphere**

3 Haofei Zhang¹, David R. Worton^{2,3}, Michael Lewandowski⁴, John Ortega⁵, Caitlin L.
4 Rubitschun¹, Kasper Kristensen⁶, Pedro Campuzano-Jost^{7,8}, Douglas A. Day^{7,8}, Jose L.
5 Jimenez^{7,8}, Mohammed Jaoui⁹, John H. Offenberg⁴, Tadeusz E. Kleindienst⁴, Jessica
6 Gilman^{7,10}, William C. Kuster^{7,10}, Joost de Gouw^{7,10}, Changhyoun Park¹¹, Gunnar W.
7 Schade¹¹, Amanda A. Frossard¹², Lynn Russell¹², Lisa Kaser¹³, Werner Jud¹³, Armin
8 Hansel¹³, Luca Cappellin⁵, Thomas Karl⁵, Marianne Glasius⁶, Alex Guenther⁵, Allen H.
9 Goldstein^{2,14}, John H. Seinfeld¹⁵, Avram Gold¹, Richard M. Kamens¹, and Jason D.
10 Surratt^{1,*}

11 ¹Department of Environmental Sciences and Engineering, Gillings School of Global Public
12 Health, The University of North Carolina at Chapel Hill, Chapel Hill, NC, 27599, USA.

13 ²Department of Environmental Science, Policy and Management, University of California,
14 Berkeley, CA, 94720, USA.

15 ³Aerosol Dynamics Inc., Berkeley, CA, 94710, USA.

16 ⁴US Environmental Protection Agency, Office of Research and Development, National
17 Exposure Research Laboratory, Research Triangle Park, NC, 27711, USA.

18 ⁵National Center for Atmospheric Research, Atmospheric Chemistry Division, Boulder,
19 CO, 80301, USA.

20 ⁶Department of Chemistry, Aarhus University, 8000 Aarhus C, Denmark.

21 ⁷Cooperative Institute for Research in Environmental Sciences, University of Colorado,
22 Boulder, CO, 80309, USA.

23 ⁸Department of Chemistry and Biochemistry, University of Colorado, Boulder, CO, 80309,
24 USA.

25 ⁹Alion Science and Technology, P.O. Box 12313, Research Triangle Park, NC, 27709,
26 USA.

27 ¹⁰Chemical Sciences Division, NOAA Earth System Research Laboratory, Boulder, CO,
28 80305, USA.

1
2
3
4
5
6
7
8
9
10
11
12
13
14
15
16
17
18
19
20
21
22
23
24
25
26
27
28
29
30
31
32
33
34
35
36
37
38
39
40
41
42
43
44
45
46
47
48
49
50
51
52
53
54
55
56
57
58
59
60

29 ¹¹Department of Atmospheric Sciences, Texas A&M University, College Station, TX,
30 77843, USA.

31 ¹²Scripps Institution of Oceanography, University of California, San Diego, La Jolla, CA,
32 92093, USA.

33 ¹³Institute of Ion Physics and Applied Physics, University of Innsbruck, Innsbruck,
34 Austria.

35 ¹⁴Department of Civil and Environmental Engineering, University of California, Berkeley,
36 CA, 94720, USA.

37 ¹⁵Department of Chemical Engineering, California Institute of Technology, Pasadena, CA,
38 91125, USA.

39 *Corresponding Author: Jason D. Surratt (surratt@unc.edu)

40

41 For submission to: Environmental Science & Technology

1
2
3 **42 Abstract**
4

5
6 43 2-methyl-3-buten-2-ol (MBO) is an important biogenic volatile organic compound
7
8 44 (BVOC) emitted by pine trees and a potential precursor of atmospheric secondary organic
9
10 45 aerosol (SOA) in forested regions. In the present study, hydroxyl radical (OH)-initiated
11
12 46 oxidation of MBO was examined in smog chambers under varied initial nitric oxide (NO)
13
14 47 and aerosol acidity levels. Results indicate measurable SOA from MBO under low-NO
15
16 48 conditions. Moreover, increasing aerosol acidity was found to enhance MBO SOA.
17
18 49 Chemical characterization of laboratory-generated MBO SOA reveals that an
19
20 50 organosulfate species ($C_5H_{12}O_6S$, MW 200) formed and was substantially enhanced with
21
22 51 elevated aerosol acidity. Ambient fine aerosol ($PM_{2.5}$) samples collected from the
23
24 52 BEARPEX campaign during 2007 and 2009, as well as from the BEACHON-RoMBAS
25
26 53 campaign during 2011, were also analyzed. The MBO-derived organosulfate characterized
27
28 54 from laboratory-generated aerosol was observed in $PM_{2.5}$ collected from these campaigns,
29
30 55 demonstrating that it is a molecular tracer for MBO-initiated SOA in the atmosphere.
31
32 56 Furthermore, mass concentrations of the MBO-derived organosulfate are well correlated
33
34 57 with MBO mixing ratio, temperature, and acidity in the field campaigns. Importantly, this
35
36 58 compound accounted for an average of 0.25% and as high as 1% of the total organic
37
38 59 aerosol mass during BEARPEX 2009. An epoxide intermediate generated under low-NO
39
40 60 conditions is tentatively proposed to produce MBO SOA.
41
42
43
44
45
46
47
48
49
50
51
52
53
54
55
56
57
58
59
60

1. Introduction

Biogenic volatile organic compounds (BVOCs) are important precursors of secondary organic aerosol (SOA) in the atmosphere^{1,2}. Current studies have focused on biogenic SOA formation from isoprene, monoterpenes, and sesquiterpenes owing to their large global emission rates^{1,3,4}. 2-Methyl-3-buten-2-ol (MBO) is an oxygenated BVOC emitted by certain coniferous tree species^{5,6}. Although the global emission rate of MBO is much lower than the other BVOCs⁷, it can be highly abundant in certain regions such as pine forests of the western United States^{5,8,9}. Due to the high volatility of MBO oxidation products, it is generally not considered as a source of SOA. However, recent studies have examined the potential of MBO for producing SOA and concluded that it can marginally contribute to SOA formation under certain atmospheric conditions¹⁰⁻¹³.

In the troposphere, MBO can react with hydroxyl radicals ($k_{\text{OH}}=5.6\times 10^{-11}$ molecule⁻¹cm³s⁻¹)¹⁰, ozone ($k_{\text{O}_3}=8.3\times 10^{-18}$ molecule⁻¹cm³s⁻¹)¹⁰, and nitrate radicals ($k_{\text{NO}_3}=1.2\times 10^{-14}$ molecule⁻¹cm³s⁻¹)¹⁴. Assuming the average tropospheric concentrations of OH (1.5×10^6 molecules cm⁻³), O₃ (7×10^{11} molecules cm⁻³), and NO₃ (4.8×10^8 molecules cm⁻³)¹⁵, the estimated lifetimes of MBO reacting with these three oxidants are 3.3 h, 47.8 h, and 48.2 h, respectively. Studies have reported SOA formation from MBO initiated by these oxidants^{10,11,13,16}. Chan et al.¹¹ and Jaoui et al.¹³ investigated OH-initiated oxidation of MBO under different NO conditions. They both found that in the presence of NO, MBO does not form SOA. However, with the absence of NO, slight SOA formation was observed at SOA yields less than 1%. Jaoui et al.¹³ observed 2,3-dihydroxyisopentanol (DHIP) as a MBO SOA tracer from both low-NO chamber experiments and atmospheric particulate matter (PM) samples using the GC/MS technique. In addition, MBO oxidation could produce glycolaldehyde at a high yield under both high- and low-NO

1
2
3 85 conditions^{10,17,18}. Glycolaldehyde and its oxidation product, glyoxal, are both water-soluble
4
5
6 86 and could produce SOA on wet aerosols and clouds¹⁹⁻²¹.
7

8
9 87 Recent studies have proposed that organosulfates are an important class of SOA
10
11 88 species, especially for biogenic SOA²²⁻²⁸. Isoprene- and monoterpene-derived
12
13 89 organosulfates have been confirmed using the liquid chromatography/electrospray
14
15 90 ionization mass spectrometry (LC/ESI-MS) technique²²⁻²⁸. These organosulfate species
16
17 91 have been identified as important atmospheric SOA tracers representing biogenic SOA
18
19 92 enhanced by anthropogenic emissions of NO_x and SO₂^{2,29-32}. Moreover, aerosol acidity was
20
21 93 found to enhance SOA formation from some BVOCs (e.g., isoprene, α-pinene, and β-
22
23 94 caryophyllene) as well as the organosulfate component^{22-28,33-35}. With a structure similar to
24
25 95 isoprene, MBO may also produce organosulfates and SOA formation may be affected by
26
27 96 aerosol acidity in a similar manner. In the present study, aerosol samples were collected
28
29 97 from both MBO photooxidation chamber experiments and field campaigns in locations
30
31 98 with abundant MBO emissions. Ultra performance liquid chromatography/electrospray
32
33 99 ionization high-resolution quadrupole time-of-flight mass spectrometry (UPLC/(-)ESI-
34
35 100 HR-Q-TOFMS) was used to analyze the filter samples and hence quantitatively investigate
36
37 101 the organosulfate formation from MBO photooxidation in the atmosphere.
38
39
40
41
42

43 102 2. Experimental Section

44
45
46 103 **High-NO Chamber Experiments.** Two initially high-NO experiments (UNC1 and
47
48 104 UNC2 in Table 1) with neutral versus acidified sulfate seed aerosols were conducted on
49
50 105 the same day at the University of North Carolina 274-m³ dual outdoor smog chamber
51
52 106 facility (Pittsboro, NC) under natural sunlight. The detailed chamber instrumentation has
53
54 107 been described elsewhere³⁶⁻³⁹. Briefly, the smog chamber is divided by a Teflon film
55
56 108 curtain into two individual chambers with the same volume (~136 m³). For the neutral
57
58 109 seeded experiment, 0.06 M (NH₄)₂SO₄ solution was atomized into one chamber; 0.6 M
59
60

1
2
3 110 ((NH₄)₂SO₄ + H₂SO₄) solution was used instead in the other chamber for the acidic seeded
4
5 111 experiment. Despite the different solution concentrations, similar initial seed aerosol mass
6
7 112 concentrations were obtained in both experiments by varying the injection time. NO was
8
9 113 injected into the chambers from a high-pressure gas cylinder as soon as seed aerosol
10
11 114 volume concentrations stabilized. High-purity liquid MBO (>98%, Aldrich) was then
12
13 115 heated in a U-tube and flushed into the chamber with a N₂ flow. MBO concentration was
14
15 116 measured using a GC/FID. Particle size distributions and the volume concentrations were
16
17 117 measured using a scanning mobility particle sizer (SMPS) (TSI 3080) coupled with a
18
19 118 condensation particle counter (CPC) (TSI 3022A). Aerosol filter samples (PALL Life
20
21 119 Sciences, Quartz, 47-mm diameter, 1.0- μ m pore size) were collected during the whole
22
23 120 photochemical period at a flow rate \sim 17 L min⁻¹ for each experiment.
24
25
26
27
28

29 121 **Low-NO Chamber Experiments.** A dynamic experiment with four stages (EPA1–
30
31 122 EPA4 in Table 1) was conducted at the U.S. EPA (Research Triangle Park, NC) 14.5-m³
32
33 123 Teflon chamber operated in a flow mode to produce a steady-state condition. There was no
34
35 124 NO added to the chamber during the experiment. The photolysis of hydrogen peroxide
36
37 125 (H₂O₂) was used as the source of OH radicals. The concentration of MBO throughout the
38
39 126 four stages was held at a constant 15 ppmC. The concentration of H₂O₂ was maintained at
40
41 127 \sim 9 ppm and RH was less than 5% during the whole experiment. The aerosol acidity was
42
43 128 changed between stages by adjusting the fraction of (NH₄)₂SO₄ and H₂SO₄ in the seed
44
45 129 aerosol (shown in Table 1). Particle organic carbon concentrations were measured by a
46
47 130 semi-continuous elemental carbon-organic carbon (EC-OC) instrument (Sunset
48
49 131 Laboratories, Tigard, OR). Aerosol samples were collected at a flow rate of 15 L min⁻¹ by
50
51 132 47-mm Teflon filters for determination of the hydrogen ion concentration ([H⁺]_{air}) as nmol
52
53 133 H⁺ m⁻³ using an Oakton 300 pH probe (Vernon Hills, IL) after dissolution in 10 mL of
54
55 134 distilled deionized water. Teflon impregnated glass fiber filters (47 mm; Pall Gelman
56
57
58
59
60

1
2
3 135 Laboratory, Ann Arbor, MI) were used for other off-line chemical determinations. The
4
5 136 detailed gas-phase and aerosol-phase measurements have been described elsewhere^{13,34}.

7
8 137 **Field Measurements – the BEARPEX Campaigns.** The BEARPEX (Biosphere
9
10 138 Effects on Aerosols and Photochemistry Experiment) campaigns were conducted at a
11
12 139 ponderosa pine plantation located between Sacramento and Lake Tahoe in the Sierra
13
14 140 Nevada Mountains, California^{40,41}. MBO is one of the dominant biogenic VOCs emitted by
15
16 141 the forest at the BEARPEX site^{8,42,43}. The field data used for this study were collected from
17
18 142 September 20 – 25, 2007, and July 25 – 30, 2009. The two sampling periods were
19
20 143 characterized by very different conditions; 2007 was cooler and wetter while 2009 was
21
22 144 hotter and drier. A high-resolution time-of-flight aerosol mass spectrometer (HR-ToF-
23
24 145 AMS, Aerodyne Research Inc., hereinafter AMS for short) was used during the BEARPEX
25
26 146 2007 campaign to measure non-refractory PM₁ aerosol components, from which the mass
27
28 147 concentrations of individual components (sulfate, nitrate, ammonium, chloride, and
29
30 148 organics) were resolved⁴⁴. The AMS operation at BEARPEX was described by Farmer et
31
32 149 al.⁴⁵. In the BEARPEX 2009 campaign, the PM₁ organic mass was measured by FTIR and
33
34 150 sulfate, nitrate, and ammonium were measured using a Metrohm ion chromatograph
35
36 151 equipped with a Metrosep A Supp 5 column for anions and a Metrosep C 4 column for
37
38 152 cations. The average organic mass concentrations were ~ 2.3 μg m⁻³ and ~3.7 μg m⁻³
39
40 153 during 2007 and 2009, respectively. Aerosol acidities (strong acidity) were estimated based
41
42 154 on charge balance using the measured concentrations of the three inorganic components.
43
44 155 Average acidities were estimated by averaging for each filter sampling period. MBO and
45
46 156 isoprene were measured by two different in situ instruments; in 2007 using GC/MS
47
48 157 operated by the National Oceanic and Atmospheric Administration (NOAA)^{9,46} and in
49
50 158 2009 using GC/FID operated by Texas A&M University^{47,48}.

51
52
53
54
55
56
57
58
59
60 159 PM_{2.5} samples were collected using high-volume samplers during the two continuous

1
2
3 160 five-day periods in 2007 and 2009, with three filters each day, to provide sufficient time
4
5
6 161 resolution to examine the diurnal variation of aerosol compositions. This filter sampling
7
8 162 approach could also separate the influence of local biogenic emissions in the morning from
9
10 163 the anthropogenic emissions from the California Central Valley arriving in the afternoon
11
12
13 164 and subsequent nighttime chemistry.

15 165 **Field Measurements – the BEACHON-RoMBAS Campaign.** The BEACHON-
16
17 166 RoMBAS (Bio-hydro-atmosphere interactions of Energy, Aerosols, Carbon, H₂O,
18
19 167 Organics & Nitrogen – Rocky Mountain Biogenic Aerosol Study) campaign was
20
21
22 168 conducted from July – August, 2011 at the Manitou Forest Observatory located in Pike
23
24 169 National Forest, Colorado. Site information has been described elsewhere^{49,50}. The
25
26
27 170 BEACHON-RoMBAS site was chosen due to abundant BVOC emissions, in which the
28
29 171 MBO emission is important, but with limited anthropogenic influence.

31 172 Measurements of aerosol components were performed using a high-resolution AMS⁴⁴.
32
33
34 173 The sum of MBO and isoprene was measured using two Proton-Transfer-Reaction Time-
35
36 174 of-Flight Mass Spectrometers (PTR-TOF-MS, Ionicon Analytik GmbH, Austria and
37
38 175 University of Innsbruck). Details about the instruments and data evaluation can be found in
39
40
41 176 Jordan et al.⁵¹, Graus et al.⁵², Müller et al.⁵³ and Cappellin et al.⁵⁴. Ambient air was
42
43 177 sampled at a flow rate of ~9 SLPM through a 40m long Teflon (PFA) line (1/4" OD)
44
45 178 mounted at 25.1 m on the canopy tower. Both instruments were sampling of the same line
46
47 179 with a sampling period of about 10 s. The merged dataset was averaged to 6 min. The drift
48
49 180 tube was operated at 2.3 mbar (both instruments) and a drift voltage of a drift voltage of
50
51 181 580 V (UIBK) and 550 V (NCAR) and a drift tube temperature of 60C (both instruments).
52
53 182 Calibration was performed by dynamically diluting VOC standards at ppmV levels with
54
55 183 scrubbed air. During BEACHON-RoMBAS, the average temperature (~17°C) and the
56
57 184 organic aerosol mass (~ 1.4 µg m⁻³) were fairly low; therefore, a 72 h-integrated aerosol
58
59
60

1
2
3 185 filter sampling approach with a flow rate of $1 \text{ m}^3 \text{ min}^{-1}$ was performed using a high volume
4
5 186 sampler to collect sufficient aerosol mass on each filter. The average acidity for each filter
6
7
8 187 sampling period was estimated in the same manner as the BEARPEX 2007.
9

10 **Filter Sample Extractions and Chemical Analyses.** Filters collected from chamber
11
12 188 experiments and field campaigns were stored in individual pre-cleaned packets in a -20°C
13
14 189 freezer before extraction. All filters were extracted in 15 mL of high-purity methanol (LC-
15
16 190 MS CHROMASOLV-grade, Sigma-Aldrich) by sonication for 45 min. The methanol
17
18 191 extracts were then blown dry under a gentle N_2 stream at ambient temperature²⁴. Soot
19
20 192 particles and quartz fibers for all filter extracts were removed using procedures outlined
21
22 193 in²⁴. Dried residues from filter extracts were reconstituted with 150 μL of 50:50 (v/v)
23
24 194 solvent mixture of 0.1% acetic acid in methanol (LC-MS ChromaSolv-Grade, Sigma-
25
26 195 Aldrich) and 0.1% acetic acid in water (LC-MS ChromaSolv-Grade, Sigma-
27
28 196 Aldrich) and 0.1% acetic acid in water (LC-MS ChromaSolv-Grade, Sigma-Aldrich). The
29
30 197 resultant mixtures were then shaken and sonicated for 5 min and then stored at -20°C
31
32 198 before analyses. The detailed description of the UPLC/(-)ESI-HR-Q-TOFMS technique
33
34 199 and operating conditions can be found in Zhang et al.³⁸. Propyl sulfate was selected as the
35
36 200 surrogate standard for quantifying the MBO-derived organosulfate owing to the similar
37
38 201 solubility and retention time³⁵. The detection limit is $\sim 0.05 \text{ ng}$ for this surrogate standard.
39
40
41
42

43 202 **3. Results and Discussion**

44
45
46 203 **Effects of NO and Acidity on SOA Yields from MBO Photooxidation.** Figure 1
47
48 204 shows the results of the initially high-NO experiments conducted at the UNC dual outdoor
49
50 205 smog chambers on the same day. Similar gas-phase conditions were obtained for both
51
52 206 experiments (Figure 1a) and the only variation between the two experiments was the
53
54 207 different sulfate seed aerosol acidities. Figure 1b represents the particle volume
55
56 208 concentrations (wall loss uncorrected) of the two MBO experiments compared to seed
57
58 209 aerosol only experiments without MBO. Slight SOA formation ($\sim 7 \mu\text{g m}^{-3}$) was observed
59
60

1
2
3 210 only in the acidic experiment and the SOA decreased rapidly after reaching the maximum.
4
5 211 It should be noted that the SOA was not formed until after the NO concentration
6
7
8 212 approached zero, when half of the initial MBO (~ 2 ppmC) remained and its peroxy
9
10 213 radicals likely began to react with hydroperoxy radicals (RO_2+HO_2) and/or other peroxy
11
12 214 radicals (RO_2+RO_2).

15 215 As shown in Table 1, for the low-NO experiment conducted at the EPA smog
16
17 216 chamber, measureable SOA was formed in all the four stages with SOA yields up to 1%.
18
19 217 In these acidity-varied experiments $[\text{H}^+]_{\text{air}}$ ranged from 125 – 1587 nmol m^{-3} and the SOA
20
21 218 formation during each stage correlated well with increasing acidity. Figure 2 shows the
22
23 219 relationship between the change (%) of organic carbon (OC) concentration compared to
24
25 220 the neutral seed case and measured aerosol acidity ($[\text{H}^+]_{\text{air}}$ nmol m^{-3}) for different BVOCs.
26
27 221 The data of isoprene, α -pinene, and β -caryophyllene are reproduced from Surratt et al.²³
28
29 222 and Offenberg et al.³⁴. In these prior studies, SOA formation from isoprene, β -
30
31 223 caryophyllene, and α -pinene was found to correlate with aerosol acidity as a linear
32
33 224 relationship, however, with different slopes. From the present work, the MBO case does
34
35 225 also follow the same trend with a slope larger than that of α -pinene and lower than those of
36
37 226 isoprene and β -caryophyllene. It should be noted that the previous studies were performed
38
39 227 under $\text{RH} < 30\%$, but this study uses $\text{RH} < 5\%$, likely causing the aerosols to be more acidic
40
41 228 and suggests the acidity effect of MBO may be weaker than this figure indicates compared
42
43 229 to the other three BVOCs.
44
45
46
47
48
49

50 230 By combining the two sets of smog chamber experiments, SOA was found to form
51
52 231 only when NO was not present, that is, SOA was probably formed from the RO_2+HO_2
53
54 232 channel and/or the RO_2+RO_2 channel. In addition, the formation of MBO SOA under low-
55
56 233 NO conditions was likely enhanced with greater acidity, similar as the observation for the
57
58 234 other BVOCs, such as isoprene²³, β -caryophyllene³⁴, and α -pinene³⁴.

1
2
3
4 235 **Organosulfate Formation from MBO Photooxidation.** Filter samples collected
5
6 236 from all the chamber experiments discussed above were analyzed using UPLC/(-)ESI-HR-
7
8 237 Q-TOFMS. The results suggest an organosulfate species was produced from all the
9
10 238 experiments. Accurate mass data suggest that the MBO-derived organosulfate has a
11
12 239 molecular formula of C₅H₁₂O₆S (MW 200.0355). Figure 3a shows the tandem mass spectra
13
14 240 (MS² spectra) of this organosulfate (*m/z* 199) from the low-NO experiments. The most
15
16 241 abundant fragment is *m/z* 97, which indicates the presence of a sulfate ester group in this
17
18 242 compound (-OSO₃H)²². Since this organosulfate species has the same carbon number (5) as
19
20 243 MBO, it likely maintains the backbone of MBO. Thus, its tentative isomeric structures are
21
22 244 proposed in Figure 3a. From a recent study by Jaoui et al.¹³, another SOA tracer (DHIP,
23
24 245 MW 120), with a similar structure to our proposed organosulfate (i.e., the sulfate ester
25
26 246 group is substituted by a hydroxyl group), was observed by GC/MS analyses. For a similar
27
28 247 biogenic hydrocarbon, isoprene, previous studies have found that its three major SOA
29
30 248 tracers, the 2-methyltetrols (MW 136) and a C₅ organosulfate species (MW 216), are both
31
32 249 derived from the same intermediate compound (i.e., isoprene epoxydiols, or IEPOX)^{25,35,55}.
33
34 250 Similarly, it is likely that both DHIP and the MBO-derived organosulfate found in the
35
36 251 present study are formed from an epoxide intermediate, especially since reactive uptake of
37
38 252 epoxides has been shown to be kinetically feasible in forming organosulfates and polyols
39
40 253 under tropospheric conditions⁵⁶. The potential mechanism is discussed further below.

41
42 254 Moreover, it is observed that the mass concentrations of the MBO-derived
43
44 255 organosulfate also correlated well with acidity (R²=0.87), as shown in Table 1 (and Figure
45
46 256 S1). This finding is consistent with previous observations of organosulfates derived from
47
48 257 other BVOCs²²⁻²⁴. This may suggest the formation mechanism of the MBO-derived
49
50 258 organosulfate is similar to that of the other organosulfates. Furthermore, increased acidity
51
52 259 tends to promote both OC and the MBO-derived organosulfate formation to a similar
53
54
55
56
57
58
59
60

1
2
3 260 extent (Figure S1), suggesting that the same mechanism may result in the organosulfate
4
5 261 and bulk SOA formation. The $C_5H_{12}O_6S$ organosulfate is also well correlated with OC
6
7 262 ($R^2=0.96$), indicating the MBO-derived organosulfate can serve as a good tracer for the OC
8
9 263 concentrations.

10
11
12 264 **Field Observations of the MBO-Derived Organosulfate.** In addition to the chamber
13
14 265 results, the MBO-derived organosulfate was also observed in ambient field samples. In the
15
16 266 chemical analyses using UPLC/(-)ESI-HR-Q-TOFMS the same organosulfate species were
17
18 267 observed at m/z 199 from BEARPEX 2007, 2009, and BEACHON-RoMBAS 2011
19
20 268 campaigns. The MS^2 spectra and retention times of the m/z 199 organosulfate from the
21
22 269 field campaigns are identical to those from MBO chamber experiments (Figure 3b),
23
24 270 confirming that the m/z 199 organosulfate observed from field campaigns was likely
25
26 271 derived from MBO.

27
28
29 272 Figure 4a shows the averaged MBO mixing ratio and MBO-derived organosulfate
30
31 273 mass concentration during each filter-sampling period from BEARPEX 2009. The diurnal
32
33 274 variation of the organosulfate mass concentrations is generally consistent with that of
34
35 275 MBO mixing ratios. Both the MBO mixing ratio and the MBO-derived organosulfate
36
37 276 concentration consistently fell to much lower levels at night. It should be noted that
38
39 277 sometimes the MBO mixing ratios in the morning were similar or even higher than the
40
41 278 afternoon, but the MBO organosulfate was still higher in the afternoon. This is probably
42
43 279 because: (1) there will be a certain time delay to form an organosulfate from MBO; (2) the
44
45 280 OH and O_3 concentrations were highest in the afternoon which likely increased the
46
47 281 organosulfate production rate; (3) the factors that enhance organosulfate formation such as
48
49 282 aerosol acidity are higher in the afternoon when the relative humidity dropped to lower
50
51 283 levels and the urban emissions arrived (See Figure 5b). Figure 4b shows the time series of
52
53 284 isoprene mixing ratios and the IEPOX-derived organosulfate mass concentrations. The
54
55
56
57
58
59
60

1
2
3 285 comparison between Figures 4a and 4b suggests that both the isoprene mixing ratio and the
4
5 286 IEPOX-derived organosulfate concentration did not follow the diurnal pattern as the MBO
6
7 287 did at the BEARPEX site; especially for the IEPOX-derived organosulfates which
8
9 288 accumulated to higher concentrations at the end of the week, rather than being dominated
10
11 289 by the diurnal trend. At the BEARPEX site, MBO is locally emitted, but isoprene is
12
13 290 emitted upwind of the site⁴¹. Thus, the IEPOX-derived organosulfate likely formed upwind
14
15 291 with the urban plume before it arrived at the site. Hence, the measured IEPOX-derived
16
17 292 organosulfate cannot be simply explained by the trends in local emissions. In some
18
19 293 previous studies, the IEPOX-derived organosulfate was found to be the most abundant
20
21 294 organosulfate species from ambient aerosols^{29,31,32}. However, at the BEARPEX site, the
22
23 295 MBO organosulfate has similar abundance as the IEPOX-derived organosulfate. The
24
25 296 MBO-derived organosulfate alone can account for an average of 0.25% and as high as 1%
26
27 297 of measured organic PM₁ at BEARPEX 2009 (Table S2). The comparison between the
28
29 298 MBO-derived and the IEPOX-derived organosulfates further demonstrates that the two C₅
30
31 299 organosulfate species arose from different sources and the MBO organosulfate could be a
32
33 300 substantial SOA component locally.

301 Figures 5 a-c examine the relationship between the MBO-derived organosulfate
302 concentrations and temperatures, aerosol acidities, and MBO mixing ratios from the
303 BEARPEX and BEACHON-RoMBAS campaigns. Temperatures, aerosol acidities, and
304 MBO mixing ratios were averaged for each filter-sampling period. All the BEARPEX
305 2009 data are much higher than the other two campaigns and have a larger dependence on
306 sampling time during the day. Thus, the correlations analyzed at different times of day
307 (i.e., morning, afternoon, and night) are shown separately for the BEARPEX 2009 data.
308 The temperature during BEARPEX 2007 and BEACHON-RoMBAS are both lower than
309 that of BEARPEX 2009 (Figure 5a). For BEARPEX 2009, the temperature during the

1
2
3 310 daytime is much higher than that during the nighttime but the temperatures in the morning
4
5 311 and afternoon are generally similar. Similar to the temperature conditions, the aerosol
6
7 312 acidities during BEARPEX 2007 and BEACHON-RoMBAS are also significantly lower
8
9 313 (by an order of magnitude) than those during BEARPEX 2009. Additionally, during
10
11 314 BEARPEX 2009 the aerosol acidity is substantially enhanced (by a factor of 3 as shown in
12
13 315 Figure 5b) in the afternoon, likely due to the arrival of urban emissions and lower relative
14
15 316 humidity. In general, the MBO-derived organosulfate concentration correlates well with
16
17 317 the average aerosol acidity (represented as $[H^+]_{\text{air}}$ in nmol/m^3 in Figure 5b, $R^2=0.68$). As
18
19 318 shown in Figure 5c, the MBO-derived organosulfate concentration correlates well with the
20
21 319 average MBO mixing ratio ($R^2=0.75$). The MBO mixing ratios increase with increasing
22
23 320 temperature owing to the MBO emissions being strongly sensitive to temperature⁶.
24
25
26
27
28

29 321 Generally for the BEARPEX 2009 data, higher temperatures and MBO mixing ratios
30
31 322 explain the increased formation of organosulfate in the morning compared to the
32
33 323 nighttime; the higher acidity partly explains the further enhancement of organosulfate
34
35 324 formation in the afternoon compared to the other periods in 2009. The BEACHON-
36
37 325 RoMBAS results are similar to the BEARPEX 2007 results in terms of the lower
38
39 326 temperatures, aerosol acidities, and MBO mixing ratios. Although the BEACHON-
40
41 327 RoMBAS data show slightly higher MBO mixing ratios, the MBO organosulfate formation
42
43 328 was not enhanced at the BEACHON-RoMBAS site compared to the BEARPEX 2007
44
45 329 results. One possible explanation might be that under low aerosol acidity, the formation of
46
47 330 MBO organosulfate is generally low and not well correlated with MBO mixing ratio.
48
49 331 Another possibility is that the sum of MBO and isoprene was measured from BEACHON-
50
51 332 RoMBAS and 80% was estimated to be MBO, which might be over estimated. Overall, the
52
53 333 field data shown in Figure 5 clearly suggest that MBO is the precursor of this
54
55 334 organosulfate species, which is substantially enhanced as aerosol acidity increases.
56
57
58
59
60

1
2
3
4 335 **Potential Mechanisms for Atmospheric MBO SOA Formation.** The mechanisms
5
6 336 by which MBO-derived organosulfate and other SOA tracers¹³ form in the atmosphere are
7
8 337 still unclear. However, there are a few potential mechanisms that may lead to MBO SOA
9
10 338 formation. Chan et al.¹¹ has proposed the RO₂+RO₂ reaction could produce DHIP, which
11
12 339 was observed from the MBO low-NO experiments by Jaoui et al.¹³. However, the
13
14 340 formation of the *m/z* 199 organosulfate is unlikely via this pathway, since the esterification
15
16 341 of an alcohol (i.e., DHIP) and sulfuric acid forming an organosulfate is kinetically
17
18 342 infeasible in the particle phase under either chamber conditions or ambient conditions⁵⁷.
19
20 343 Consequently, alternative reactions must explain the formation of the *m/z* 199
21
22 344 organosulfate. As discussed above, the formation pattern of the MBO-derived
23
24 345 organosulfate and DHIP is similar to that of the IEPOX-derived organosulfate and the 2-
25
26 346 methyltetrols^{25,35}. Similarly to the IEPOX chemistry, an epoxide is tentatively proposed to
27
28 347 be the intermediate (oxidation) product forming MBO-derived organosulfate as shown in
29
30 348 Scheme 1. An MBO-derived epoxide could either be produced from ozonolysis, H₂O₂
31
32 349 oxidation of MBO or from the further reaction of an MBO hydroxyhydroperoxide.
33
34 350 Therefore, an MBO-derived epoxide can form organosulfates by reacting with sulfuric acid
35
36 351 or form DHIP by hydrolysis. Epoxidation has been observed from the ozonolysis of
37
38 352 olefins^{58,59}. However, the epoxide yield from olefin ozonolysis tends to be low (<5%)⁶⁰
39
40 353 and this is likely a minor pathway in the atmosphere. Furthermore, an MBO-derived
41
42 354 hydroxyhydroperoxide is unlikely to undergo further fast OH oxidation like the isoprene
43
44 355 hydroxyhydroperoxide does because of the absence of an extra carbon-carbon double
45
46 356 bond. Liu et al.¹² have reported MBO epoxide from acid-catalyzed oxidation of MBO with
47
48 357 H₂O₂ (shown in Scheme 1). which is more likely an aqueous-phase process. Therefore,
49
50 358 more work is required to characterize the formation mechanism of the MBO-derived
51
52 359 organosulfate, as well as DHIP, in the atmosphere.
53
54
55
56
57
58
59
60

1
2
3 **Atmospheric Implications.** In the present study, MBO photooxidation is investigated
4
5 360
6 361 in both smog chamber experiments and field campaigns where MBO emissions are
7
8 362 important. SOA formation from MBO was observed under low-NO conditions and after
9
10 363 NO was reacted in the high-NO chamber experiments. Under both conditions, aerosol
11
12 364 acidity was found to promote the formation of MBO SOA. In addition, an organosulfate
13
14 365 species ($C_5H_{12}O_6S$, MW 200) was substantially enhanced as aerosol acidity increased.
15
16 366 From the BEARPEX and BEACHON-RoMBAS campaigns, a species with the same mass
17
18 367 spectrometric signature was observed to correlate well with MBO mixing ratio and aerosol
19
20 368 acidity. Moreover, the average MBO organosulfate concentration measured from the
21
22 369 BEARPEX site is similarly abundant to the IEPOX-derived organosulfate ($\sim 15 \text{ ng m}^{-3}$);
23
24 370 the latter has been reported to be the most abundant organosulfate tracer in a number of
25
26 371 areas²⁹.

27
28
29 372 This is an important finding because MBO could be a locally abundant BVOC in
30
31 373 certain regions, such as the western United States. Although the SOA yield reported in
32
33 374 previous studies is low ($<1\%$), the SOA mass concentration produced could still be
34
35 375 appreciable with the high emission rates expected at locations like the BEARPEX site. As
36
37 376 discussed above, the formation mechanism of MBO-derived organosulfate is likely similar
38
39 377 to that of the IEPOX-derived organosulfate. Lin et al.³⁵ found that the IEPOX-derived
40
41 378 organosulfate accounts for $\sim 5\%$ of total SOA from IEPOX. Assuming the same mass
42
43 379 fraction in the MBO case, MBO SOA can accounts for as high as $0.4 \mu\text{g m}^{-3}$, which is 10%
44
45 380 of total organic mass on average. However, further investigation is required to provide a
46
47 381 more accurate estimate. As a result, the inclusion of SOA formation from MBO in current
48
49 382 air quality models may be important⁶¹, especially for regional or local predictions of SOA.
50
51 383 The MBO-derived organosulfate has the potential to serve as an SOA tracer for source
52
53 384 apportionment method under further investigation. These new observations of MBO
54
55
56
57
58
59
60

1
2
3 385 organosulfate formation and the acidity effect are consistent with previous findings of the
4
5 386 organosulfate formation from other BVOCs, including isoprene and monoterpenes^{24,25,35}.
6
7

8 387 Although additional work is warranted, it is likely that the formation mechanisms of these
9
10 388 biogenic organosulfate species are similar.
11
12

13 389

14
15 390 **Acknowledgements:**
16

17 391 This study was supported by an U. S. EPA contract (EP-W-09-023) to the University
18
19 392 of North Carolina. The U.S. Environmental Protection Agency through its Office of
20
21 393 Research and Development collaborated in the research described here under Contract EP-
22
23 394 D-10-070 to Alion Science and Technology. The manuscript is subjected to external peer
24
25 395 review and has been not been cleared for publication. Mention of trade names or
26
27 396 commercial products does not constitute endorsement or recommendation. The BEARPEX
28
29 397 measurements were supported by an NSF grant ATM-0922562 to the University of
30
31 398 California, Berkeley, and ATM-0904203 to the University of California, San Diego. The
32
33 399 BEACHON-RoMBAS measurements were supported by NSF sponsorship of the National
34
35 400 Center for Atmospheric Research (NCAR). UPLC/ESI-HR-Q-TOFMS analyses were
36
37 401 conducted in the UNC-CH Biomarker Mass Facility located within the Department of
38
39 402 Environmental Sciences and Engineering, which is a part of the UNC-CH Center for
40
41 403 Environmental Health and Susceptibility and is supported by NIEHS (Grant 5P20-
42
43 404 ES10126). J. D. Surratt was supported in part by the Electric Power Research Institute
44
45 405 (EPRI). Thanks to Ying-Hsuan Lin for helping to operate the UPLC/(-)ESI-HR-Q-TOFMS
46
47 406 instrument. The meteorological measurements from BEACHON-RoMBAS were
48
49 407 performed by Andrew A. Turnipseed. The IC measurements for BEARPEX 2009 were
50
51 408 performed by M. P. Madsen. PCJ, DAD and JLJ were supported by NSF ATM-0919189
52
53 409 and DOE (BER/ASR Program) DE-SC0006035 and DE-SC0006711. Measurements
54
55
56
57
58
59
60

1
2
3
4
5
6
7
8
9
10
11
12
13
14
15
16
17
18
19
20
21
22
23
24
25
26
27
28
29
30
31
32
33
34
35
36
37
38
39
40
41
42
43
44
45
46
47
48
49
50
51
52
53
54
55
56
57
58
59
60

410 conducted by the University of Innsbruck were supported by the Austrian Science Fund
411 (FWF): Lisa Kaser is a recipient of a DOC-fFORTE-fellowship of the Austrian Academy
412 of Sciences at the Institute of Ion Physics and Applied Physics.

References

- [1] Hallquist, M.; Wenger, J. C.; Baltensperger, U.; Rudich, Y.; Simpson, D.; Claeys, M.; Dommen, J.; Donahue, N. M.; George, C.; Goldstein, A. H.; Hamilton, J. F.; Herrmann, H.; Hoffmann, T.; Iinuma, Y.; Jang, M.; Jenkin, M. E.; Jimenez, J. L.; Kiendler-Scharr, A.; Maenhaut, W.; McFiggans, G.; Mentel, Th. F.; Monod, A.; Prévôt, A. S.; Seinfeld, J. H.; Surratt, J. D.; Szmigielski, R.; Wildt, J. The formation, properties and impact of secondary organic aerosol: current and emerging issues. *Atmos. Chem. Phys.* **2009**, *9*, 5155–5236.
- [2] Hoyle, C. R.; Boy, M.; Donahue, N. M.; Fry, J. L.; Glasius, M.; Guenther, A.; Hallar, A. G.; Huff Hartz, K.; Petters, M. D.; Petäjä, T.; Rosenoern, T.; Sullivan, A. P. A review of the anthropogenic influence on biogenic secondary organic aerosol. *Atmos. Chem. Phys.* **2011**, *11*, 321–343.
- [3] Guenther, A.; Pierce, B.; Lamb, B.; Harley, P.; Fall, R. Natural emission of non-methane volatile organic compounds, carbon monoxide, and oxides of nitrogen from North America. *Atmos. Environ.* **2000**, *34*, 2205–2230.
- [4] Guenther, A.; Karl, T.; Harley, P.; Wiedinmyer, C.; Palmer, P. I.; Geron, C. Estimates of global terrestrial isoprene emissions using MEGAN (Model of Emissions of Gases and Aerosols from Nature). *Atmos. Chem. Phys.* **2006**, *6*, 3181–3210.
- [5] Goldan, P. D.; Kuster, W. C.; Fehsenfeld, F. C. The observation of a C5 alcohol emission in a North American pine forest. *Geophys. Res. Lett.* **1993**, *20*, 1039–1042.
- [6] Harley, P.; Fridd-Stroud, V.; Greenberg, J.; Guenther, A.; Vasconcellos, P. Emission of 2-methyl-3-buten-2-ol by pines: a potentially large natural source of reactive carbon to the atmosphere. *J. Geophys. Res.* **1998**, *103*, 25479–25486.
- [7] Fu, T. M.; Jacob, D. J.; Wittrock, F.; Burrows, J. P.; Vrekoussis, M.; and Henze, D. K. Global budgets of atmospheric glyoxal and methylglyoxal, and implications for formation of secondary organic aerosols. *J. Geophys. Res.* **2008**, *113*, D15303, doi: 10.1029/2007JD009505.
- [8] Lamanna, M. S.; Goldstein, A. H. In-situ measurements of C2-C10 VOCs above a Sierra Nevada ponderosa pine plantation. *J. Geophys. Res.* **1999**, *104*, D17, 21247-21262.
- [9] Bouvier-Brown, N. C.; Goldstein, A. H.; Worton, D. R.; Matross, D. M.; Gilman, J. B.; Kuster, W. C.; Welsh-Bon, D.; Warneke, C.; de Gouw, J. A.; Cahill, T. M.; Holzinger, R. Methyl chavicol: characterization of its biogenic emission rate, abundance, and oxidation products in the atmosphere, *Atmos. Chem. Phys.* **2009**, *9*, 2061–2074.
- [10] Carrasco, N.; Doussin, J. F.; O'Connor, M.; Wenger, J. C.; Picquet-Varrault, B.; Durand-Jolibois, R.; Carlier, P. Simulation chamber studies of the atmospheric oxidation of 2-methyl-3-buten-2-ol: Reaction with hydroxyl radicals and ozone under a variety of conditions. *J. Atmos. Chem.* **2007**, *56*, 33–55.
- [11] Chan, A. W.; Galloway, M. M.; Kwan, A. J.; Chhabra, P. S.; Keutsch, F. N.; Wennberg, P. O.; Flagan, R. C.; Seinfeld, J. H. Photooxidation of 2-methyl-3-buten-2-ol (MBO) as a potential source of secondary organic aerosol. *Environ. Sci. Technol.* **2009**, *43*, 4647–4652.
- [12] Liu, Z.; Ge, M.; Wang, W.; Yin, S.; Tong, S. The uptake of 2-methyl-3-buten-2-ol into aqueous mixed solutions of sulfuric acid and hydrogen peroxide. *Phys. Chem. Chem. Phys.* **2011**, *13*, 2069–2075.

- 1
2
3
4
5
6
7
8
9
10
11
12
13
14
15
16
17
18
19
20
21
22
23
24
25
26
27
28
29
30
31
32
33
34
35
36
37
38
39
40
41
42
43
44
45
46
47
48
49
50
51
52
53
54
55
56
57
58
59
60
- [13] Jaoui, M.; Kleindienst, T. E.; Offenberg, J. H.; Lewandowski, M.; Lonneman, W. A. SOA formation from the atmospheric oxidation of 2-methyl-3-buten-2-ol and its implications for PM_{2.5}. *Atmos. Chem. Phys.* **2012**, *12*, 2173–2188.
- [14] Rudich, Y.; Talukdar, R. K.; Fox, R. W.; Ravishankara, A. R. Rate coefficients for the reaction of NO₃ with a few olefins and oxygenated olefins, *J. Phys. Chem.* **1996**, *100*, 5374–5381.
- [15] Seinfeld, J. H.; Pandis, S. N. Atmospheric Chemistry and Physics, from Air Pollution to Climate Change, Second Edition. John Wiley, New York. **2006**, pp. 261 – 265.
- [16] Noda, J.; Ljungström, E. Aerosol formation in connection with NO₃ oxidation of unsaturated alcohols. *Atmos. Environ.* **2002**, *36*, 521–525.
- [17] Fantechi, G.; Jensen, N. R.; Hjorth, J.; Peeters, J. Mechanistic studies of the atmospheric oxidation of methyl butenol by OH radicals, ozone, and NO₃ radicals. *Atmos. Environ.* **1998**, *32*, 3547–3556.
- [18] Ferronato, C.; Orlando, J. J.; Tyndall, G. S. Rate and mechanism of the reaction of OH and Cl with 2-methyl-3buten-2-ol. *J. Geophys. Res.* **1999**, *103*, 25570–25586.
- [19] Liggio, J.; Li, S. M.; McLaren, R. Reactive uptake of glyoxal by particulate matter. *J. Geophys. Res.* **2005**, *110*, D10304, doi: 10.1029/2004JD005113.
- [20] Volkamer, R.; Martini, F. S.; Molina, L. T.; Salcedo, D.; Jimenez, J. L.; Molina, M. J. A missing sink for gas-phase glyoxal in Mexico City: Formation of secondary organic aerosol. *Geophys. Res. Lett.* **2007**, *34*, L19807, doi: 10.1029/2007GL030752.
- [21] Ervens, B.; Turpin, B. J.; Weber, R. J. Secondary organic aerosol formation in cloud droplets and aqueous particle (aqSOA): a review of laboratory, field and model studies. *Atmos. Chem. Phys.* **2011**, *11*, 11069–11102.
- [22] Surratt, J. D.; Kroll, J. H.; Kleindienst, T. E.; Edney, E. O.; Claeys, M.; Sorooshian, A.; Ng, N. L.; Lewandowski, M.; Jaoui, M.; Flagan, R. C.; Seinfeld, J. H. Evidence for organosulfates in secondary organic aerosol. *Environ. Sci. Technol.* **2007a**, *41*, 517–527.
- [23] Surratt, J. D.; Lewandowski, M.; Offenberg, J. H.; Jaoui, M.; Kleindienst, T. E.; Edney, E. O.; Seinfeld, J. H. Effect of acidity on secondary organic aerosol formation from isoprene. *Environ. Sci. Technol.* **2007b**, *41*, 5363–5369.
- [24] Surratt, J. D.; Gómez-González, Y.; Chan, A. W. H.; Vermeylen, R.; Shahgholi, M.; Kleindienst, T. E.; Edney, E. O.; Offenberg, J. H.; Lewandowski, M.; Jaoui, M.; Maenhaut, W.; Claeys, M.; Flagan, R. C.; Seinfeld, J. H. Organosulfate formation in biogenic secondary organic aerosol, *J. Phys. Chem. A.* **2008**, *112*, 8345–8378.
- [25] Surratt, J. D.; Chan, A. W. H.; Eddingsaas, N. C.; Chan, M.; Loza, C. L.; Kwan, A. J.; Hersey, S. P.; Flagan, R. C.; Wennberg, P. O.; Seinfeld, J. H. Reactive intermediates revealed in secondary organic aerosol formation from isoprene. *Proc. Natl. Acad. Sci. USA.* **2010**, *107*, 6640–6645.
- [26] Iinuma, Y.; Müller, C.; Böge, O.; Gnauk, T.; Herrmann, H. The formation of organic sulfate esters in the limonene ozonolysis secondary organic aerosol (SOA) under acidic conditions. *Atmos. Environ.* **2007a**, *41*, 5571–5583.
- [27] Iinuma, Y.; Müller, C.; Berndt, T.; Böge, O.; Claeys, M.; Herrmann, H. Evidence for the existence of organosulfates from β -pinene ozonolysis in ambient secondary organic aerosol. *Environ. Sci. Technol.* **2007b**, *41*, 6678–6683.

- 1
2
3
4
5
6
7
8
9
10
11
12
13
14
15
16
17
18
19
20
21
22
23
24
25
26
27
28
29
30
31
32
33
34
35
36
37
38
39
40
41
42
43
44
45
46
47
48
49
50
51
52
53
54
55
56
57
58
59
60
- [28] Iinuma, Y.; Böge, O.; Kahnt, A.; Herrmann, H. Laboratory chamber studies on the formation of organosulfates from reactive uptake of monoterpene oxides. *Phys. Chem. Chem. Phys.* **2009**, *36*, 7985–7997.
- [29] Froyd, K. D.; Murphy, S. M.; Murphy, D. M.; de Gouw, J. A.; Eddingsaas, N. C.; Wennberg, P. O. Contribution of isoprene-derived organosulfates to free tropospheric aerosol mass, *Proc. Natl. Acad. Sci. USA* **2010**, *107*, 21360–21365.
- [30] Darer, A. I.; Cole-Filipiak, N. C.; O'Connor, A. E.; Elrod, M. J. Formation and stability of atmospherically relevant isoprene-derived organosulfates and organonitrates. *Environ. Sci. Technol.* **2011**, *45*, 1895–1902.
- [31] Hatch, L. E.; Creamean, J. M.; Ault, A. P.; Surratt, J. D.; Chan, M. N.; Seinfeld, J. H.; Edgerton, E. S.; Su, Y.; Prather, K. A. Measurements of isoprene-derived organosulfates in ambient aerosols by Aerosol Time-of-Flight Mass Spectrometry – Part 1: Single particle atmospheric observations in Atlanta. *Environ. Sci. Technol.* **2011a**, *45*, 5105–5111.
- [32] Hatch, L. E.; Creamean, J. M.; Ault, A. P.; Surratt, J. D.; Chan, M. N.; Seinfeld, J. H.; Edgerton, E. S.; Su, Y.; Prather, K. A. Measurements of isoprene-derived organosulfates in ambient aerosols by Aerosol Time-of-Flight Mass Spectrometry – Part 2: Temporal variability and formation mechanisms. *Environ. Sci. Technol.* **2011b**, *45*, 8648–8655.
- [33] Jang, M.; Czoschke, N. M.; Lee, S.; Kamens, R. M. Heterogeneous atmospheric aerosol production by acid-catalyzed particle-phase reactions. *Science* **2002**, *298*, 814–817.
- [34] Offenberg, J. H.; Lewandowski, M.; Edney, E. O.; Kleindienst, T. E.; Jaoui, M. Influence of aerosol acidity on the formation of secondary organic aerosol from biogenic precursor hydrocarbons. *Environ. Sci. Technol.* **2009**, *43*, 7742–7747.
- [35] Lin, Y.-H.; Zhang, Z.; Docherty, K. S.; Zhang, H.; Budisulistiorini, S. H.; Rubitschun, C. L.; Shaw, S. L.; Knipping, E. M.; Edgerton, E. S.; Kleindienst, T. E.; Gold, A.; Surratt, J. D. Isoprene epoxydiols as precursors to secondary organic aerosol formation: acid-catalyzed reactive uptake studies with authentic compounds. *Environ. Sci. Technol.* **2012**, *46*, 250–258.
- [36] Lee, S.; Jang, M.; Kamens, R. M. SOA formation from the photooxidation of α -pinene in the presence of freshly emitted diesel soot exhaust. *Atmos. Environ.* **2004**, *38*, 2597–2605.
- [37] Leungsakul, S.; Jeffries, H. E.; Kamens, R. M. A kinetic mechanism for predicting secondary aerosol formation from the reactions of d-limonene in the presence of oxides of nitrogen and natural sunlight. *Atmos. Environ.* **2005**, *39*, 7063–7082.
- [38] Zhang, H.; Surratt, J. D.; Lin, Y.-H.; Bapat, J.; Kamens, R. M. Effect of relative humidity on SOA formation from isoprene/NO photooxidation: enhancement of 2-methylglyceric acid and its corresponding oligoesters under dry conditions. *Atmos. Chem. Phys.* **2011**, *11*, 6411–6424.
- [39] Zhang, H.; Lin, Y.-H.; Zhang, Z.; Zhang, X.; Shaw, S. L.; Knipping, E. M.; Weber, R. J.; Gold, A.; Kamens, R. M.; Surratt, J. D. Secondary organic aerosol formation from methacrolein photooxidation: Roles of NO_x level, relative humidity, and aerosol acidity. *Environ. Chem.* **2012**, doi: 10.1071/EN12004.
- [40] Goldstein, A. H.; Hultman, N. E.; Fracheboud, J. M.; Bauer, M. R.; Panek, J. A.; Xu, M.; Qi, Y.; Guenther, A. B.; Baugh, W. Effects of climate variability on the carbon dioxide, water, and sensible heat fluxes above a ponderosa pine plantation in the Sierra Nevada (CA). *Agric. Forest Meteorol.* **2000**, *101*, 113–129.

- 1
2
3
4 [41] Worton, D. R.; Goldstein, A. H.; Farmer, D. K.; Docherty, K. S.; Jimenez, J. L.;
5 Gilman, J. B.; Kuster, W. C.; de Gouw, J.; Williams, B. J.; Kreisberg, N. M.;
6 Hering, S. V.; Bench, G.; McKay, M.; Kristensen, K.; Glasius, M.; Surratt, J. D.;
7 Seinfeld, J. H. Origins and composition of fine atmospheric carbonaceous aerosol
8 in the Sierra Nevada Mountains, California, *Atmos. Chem. Phys.* **2011**, *11*, 10219–
9 10241.
- 10 [42] Schade, G. W.; Goldstein, A. H.; Gray, D. W.; Lerda, M. T. Canopy and leaf
11 level 2-methyl-3-butene-2-ol fluxes from a *ponderosa* pine plantation. *Atmos.*
12 *Environ.* **2000**, *34*, 3535–3544.
- 13 [43] Schade, G. W.; Goldstein, A. H. Fluxes of oxygenated volatile organic
14 compounds from a *ponderosa* pine plantation. *J. Geophys. Res.* **2001**, *106*, D3,
15 3111–3123.
- 16 [44] DeCarlo, P. F.; Kimmel, J. R.; Trimborn, A.; Northway, M. J.; Jayne, J. T.;
17 Aiken, A. C.; Gonin, M.; Fuhrer, T.; Docherty, K.; Worsnop, D. R.; Jimenez, J. L.
18 Field-deployable, high-resolution, time-of-flight aerosol mass spectrometer, *Anal.*
19 *Chem.* **2011**, *78*, 8281–8289.
- 20 [45] Farmer, D. K.; Kimmel, J. R.; Phillips, G.; Docherty, K. S.; Worsnop, D. R.;
21 Sueper, D.; Nemitz, E.; Jimenez, J. L. Eddy covariance measurements with high-
22 resolution time-of-flight aerosol mass spectrometry: a new approach to chemically
23 resolved aerosol fluxes, *Atmos. Meas. Tech.* **2011**, *4*, 1275–1289.
- 24 [46] Gilman, J. B.; Burkhardt, J. F.; Lerner, B. M.; Williams, E. J.; Kuster, W. C.;
25 Goldan, P. D.; Murphy, P. C.; Warneke, C.; Fowler, C.; Montzka, S. A.; Miller, B.
26 R.; Miller, L.; Oltmans, S. J.; Ryerson, T. B.; Cooper, O. R.; Stohl, A.; de Gouw,
27 J. A. Ozone variability and halogen oxidation within the Arctic and sub-Arctic
28 springtime boundary layer, *Atmos. Chem. Phys.* **2010**, *10*, 10223–10236.
- 29 [47] Park, C.; Schade, G. W.; Boedeker, I. Flux measurements of volatile organic
30 compounds by the relaxed eddy accumulation method combined with a GC-FID
31 system in urban Houston, Texas. *Atmos. Environ.* **2010**, *44*, 2605–2614.
- 32 [48] Park, C.; Schade, G. W.; Boedeker, I. Characteristics of the flux of isoprene and
33 its oxidation products in an urban area. *J. Geophys. Res.* **2011**, *116*, D21303, doi:
34 10.1029/2011JD015856.
- 35 [49] Kim, S.; Karl, T.; Guenther, A.; Tyndall, G.; Orlando, J.; Harley, P.; Rasmussen,
36 R.; Apel, E. Emission and ambient distributions of Biogenic Volatile Organic
37 Compounds (BVOC) in a *ponderosa* pine ecosystem: interpretation of PTR-MS
38 mass spectra, *Atmos. Chem. Phys.* **2010**, *10*, 1759–1771.
- 39 [50] Levin, E. J. T.; Prenni, A. J.; Petters, M. D.; Kreidenweis, S. M.; Sullivan, R. C.;
40 Atwood, S. A.; Ortega, J.; DeMott, P. J.; Smith, J. N. An annual cycle of size-
41 resolved aerosol hygroscopicity at a forested site in Colorado, *J. Geophys. Res.*
42 **2012**, doi: 10.1029/2011JD016854, in press.
- 43 [51] Jordan, A.; Haidacher, S.; Hanel, G.; Hartungen, E.; Mark, L.; Seehauser, H.;
44 Schottkowsky, R.; Sulzer, P.; Mark, T. D. A high resolution and high sensitivity
45 proton-transfer-reaction time-of-flight mass spectrometer (PTR-TOF-MS), *Int. J.*
46 *Mass Spectrom.*, **2009**, *286*, 122-128, doi: 10.1016/j.ijms.2009.07.005.
- 47 [52] Graus, M.; Müller, M.; Hansel, A. High Resolution PTR-TOF: Quantification
48 and Formula Confirmation of VOC in Real Time, *J. Am. Soc. Mass. Spectr.*, **2010**,
49 *21*, 1037-1044, doi: 10.1016/j.jasms.2010.02.006.
- 50 [53] Müller, M.; Graus, M.; Ruuskanen, T. M.; Schnitzhofer, R.; Bamberger, I.;
51 Kaser, L.; Titzmann, T.; Hortnagl, L.; Wohlfahrt, G.; Karl, T.; Hansel, A. First
52 eddy covariance flux measurements by PTR-TOF, *Atmos. Meas. Tech.*, **2010**, *3*,
53 387-395.
- 54
55
56
57
58
59
60

- 1
2
3
4 [54] Cappellin, L.; Biasioli, F.; Granitto, P. M.; Schuhfried, E.; Soukoulis, C.; Costa,
5 F.; Märk, T. D.; Gasperi, F. On data analysis in PTR-TOF-MS: From raw spectra
6 to data mining, *Sensor. Actuat. B-Chem.*, **2011**, *155*, 183-190.
- 7 [55] Paulot, F.; Crouse, J. D.; Kjaergaard, H. G.; Kürten, A.; Clair, J. M. S.;
8 Seinfeld, J. H.; Wennberg, P. O. Unexpected epoxide formation in the gas-phase
9 photooxidation of isoprene. *Science* **2009**, *325*, 730–733.
- 10 [56] Eddingsaas, N. C.; VanderVelde, D. G.; Wennberg, P. O. Kinetics and products
11 of the acid-catalyzed ring-opening of atmospherically relevant butyl epoxy
12 alcohols. *J. Phys. Chem. A* **2010**, *114*, 8106–8113.
- 13 [57] Minerath, E. C.; Casale, M. T.; Elrod, M. J. Kinetics feasibility study of alcohol
14 sulfate esterification reactions in tropospheric aerosols. *Environ. Sci. Technol.*
15 **2008**, *42*, 4410–4415.
- 16 [58] Berndt, T.; Böge, O. Catalyst-free gas-phase epoxidation of alkenes. *Chem. Lett.*
17 **2005**, *34*, 584–585.
- 18 [59] Berndt, T.; Bräsel, S. Epoxidation of a series of C₂-C₆ olefins in the gas phase.
19 *Chem. Eng. Technol.* **2009**, *32*, 1189–1194.
- 20 [60] Atkinson, R. Gas-phase tropospheric chemistry of organic compounds: a review.
21 *Atmos. Environ.* **1990**, *24A*, 1–41.
- 22 [61] Steiner, A. L.; Tonse, S.; Cohen, R. C.; Goldstein, A. H.; Harley, R. A. Biogenic
23 2-methyl-3-buten-2-ol increases regional ozone and HO_x sources. *Geophys. Res.*
24 *Lett.* **2007**, *34*, L15806, doi: 10.1029/2007GL030802.
- 25
26
27
28
29
30
31
32
33
34
35
36
37
38
39
40
41
42
43
44
45
46
47
48
49
50
51
52
53
54
55
56
57
58
59
60

Table 1. Smog Chamber Experimental Conditions.

ID ^a	MBO (ppmC)	H ₂ O ₂ (ppm)	NO (ppb)	RH (%)	[H ⁺] _{air} ^c (nmol/m ³)	seed aerosol (ug/m ³ sulfate)	Average OC (μgC/m ³)	C ₅ H ₁₂ O ₆ S ^e (ng/m ³)
UNC1	4	—	200	<30%	—	50 (AS)	—	0.95
UNC2	4	—	200	<30%	—	45 (1/2 AS + 1/2 SA)	—	1.88
EPA1	15	9	< 15 ^b	<5%	125	40 (AS ^d)	6.5	6.5
EPA2	15	9	< 15 ^b	<5%	289	35 (2/3 AS + 1/3 SA ^d)	9.6	50.4
EPA3	15	9	< 15 ^b	<5%	902	35 (1/2 AS + 1/2 SA)	11.4	53.2
EPA4	15	9	< 15 ^b	<5%	1587	32 (1/3 AS + 2/3 SA)	21.9	120.3

^a Experiments UNC1 and UNC2 are the high-NO experiments conducted at the UNC dual outdoor smog chamber; experiments EPA1-EPA4 are the low-NO experiments conducted at the EPA smog chamber. ^b The NO concentrations in EPA1-4 were not obtained, but there was no NO added to the chamber during the experiments. ^c [H⁺]_{air} is used as an indicator of acidic levels. ^d “AS” represents ammonium sulfate; “SA” represents sulfuric acid. ^e C₅H₁₂O₆S is the chemical formula of the organosulfate species discussed below.

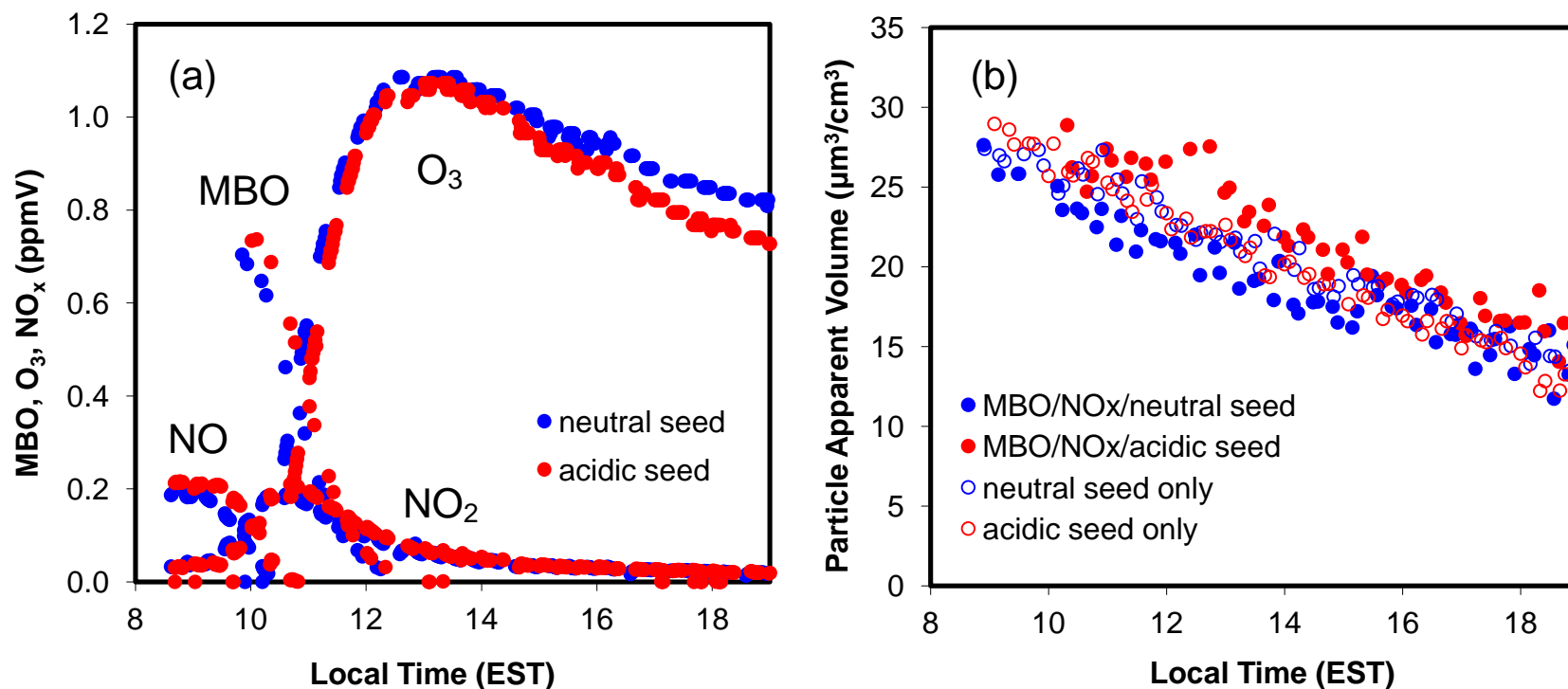


Figure 1. Online measurement results of the high-NO_x experiments (UNC1 and UNC2). (a) Time profiles of major gas-phase compounds (MBO, NO, NO₂, and O₃). (b) Wall-loss uncorrected particle apparent volume concentrations (μm³/cm³). Red solid circle represents the acidic seeded MBO experiment; blue solid circle represents the neutral seeded MBO experiments; the hollow circles in red and blue in (b) represent two control experiments with only acidic and neutral seeds, respectively.

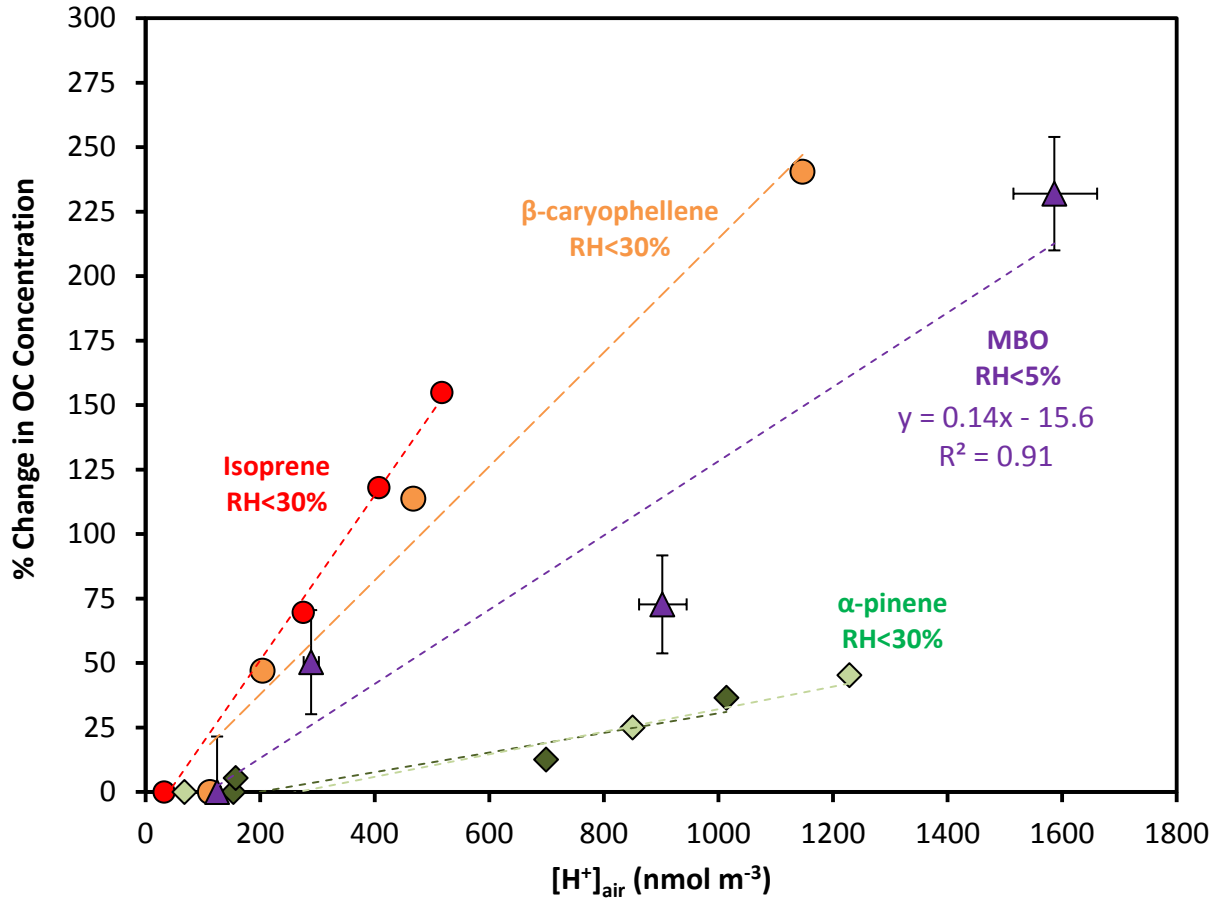


Figure 2. Relationship between the change (%) of organic carbon (OC, in $\mu\text{gC m}^{-3}$) and the measured seed aerosol acidity ($[H^+]_{\text{air}}$ nmol m⁻³) for different BVOCs. The data of isoprene, α -pinene, and β -caryophellene are reproduced from Surratt et al.²³ and Offenberg et al.³⁴. The MBO data are from the present study.

1
2
3
4
5
6
7
8
9
10
11
12
13
14
15
16
17
18
19
20
21
22
23
24
25
26
27
28
29
30
31
32
33
34
35
36
37
38
39
40
41
42
43
44
45
46
47
48
49
50
51
52
53
54
55
56
57
58
59
60

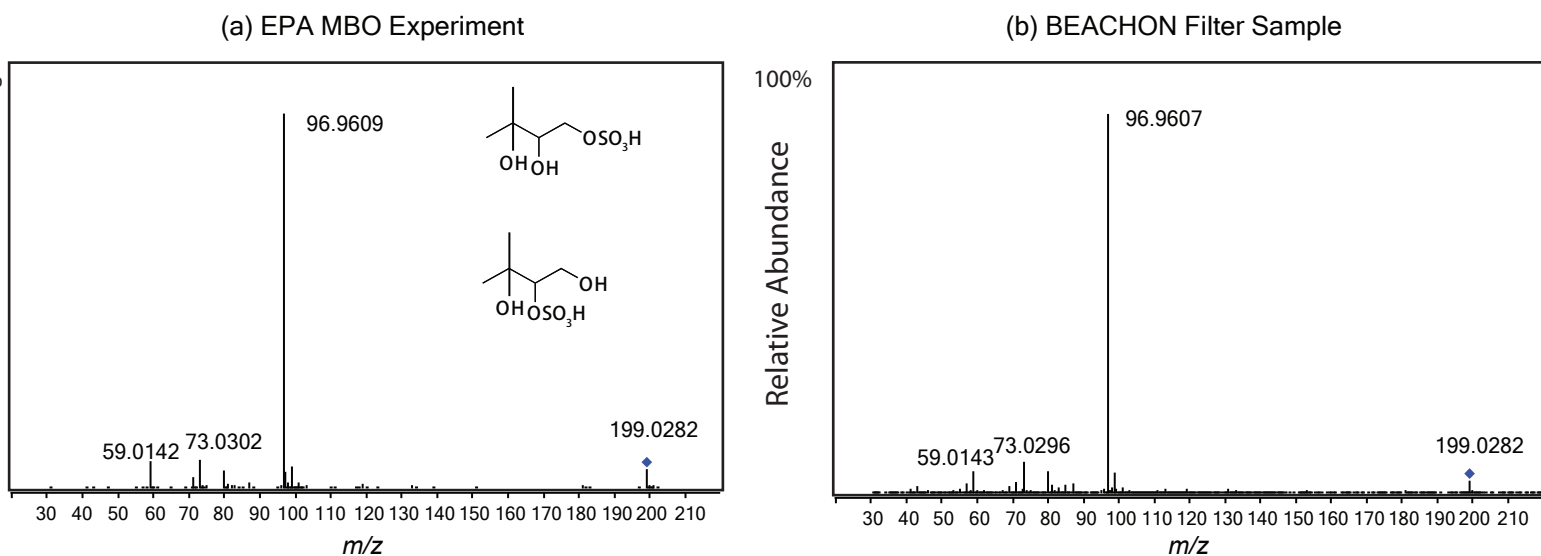


Figure 3. Tandem mass spectra (MS^2) of the MBO organosulfate (m/z 199) measured from (a) the EPA low-NO chamber experiment (EPA4, with sampled OC mass concentration $\sim 21.9 \mu\text{gC}/\text{m}^3$) and (b) the BEACHON aerosol samples. The proposed structural isomers of this organosulfate are shown in (a). The measured mass of the ion is within ± 2 mDa of the calculated mass.

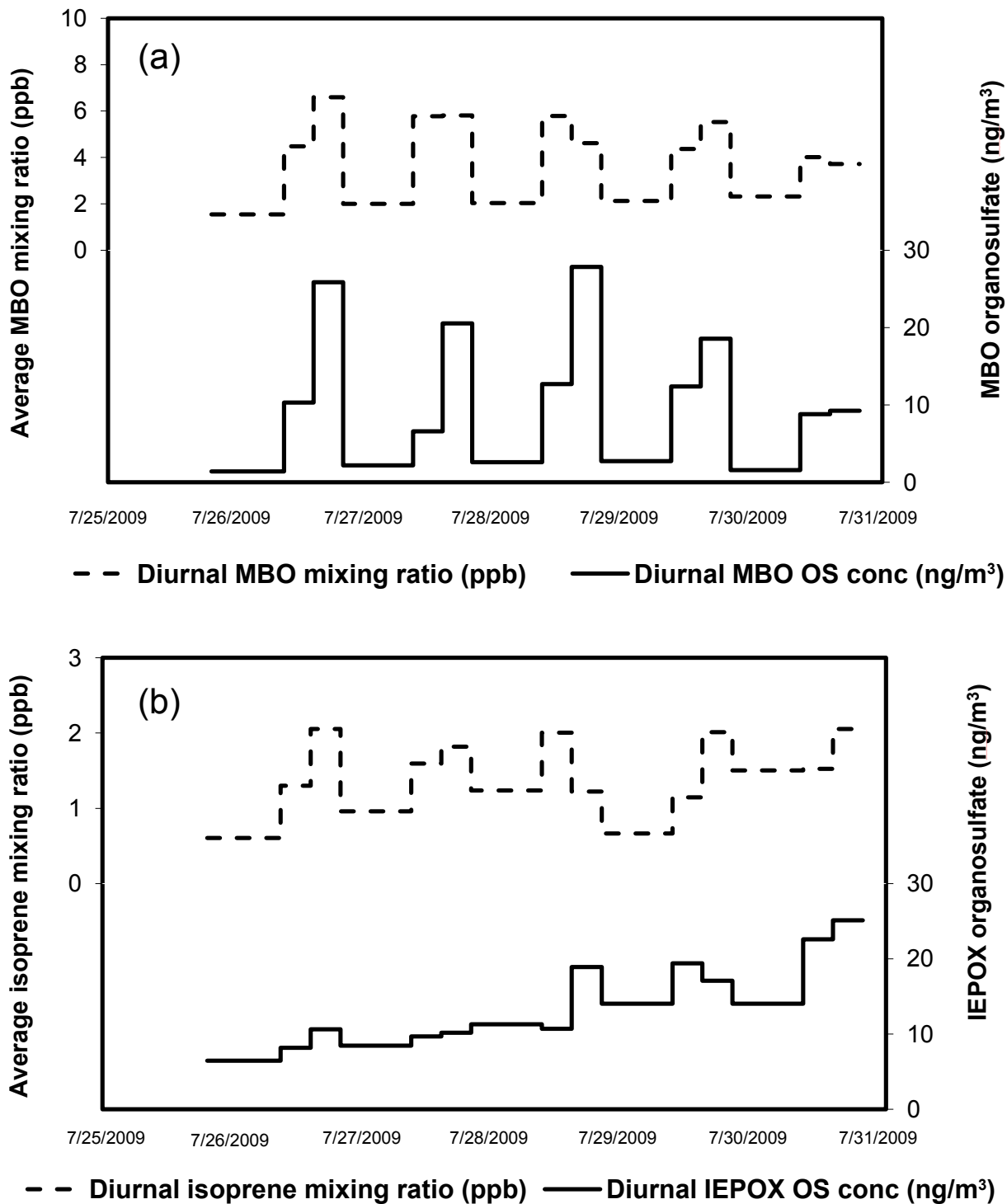


Figure 4. Comparison of diurnal variation of organosulfates and their precursors during the 2009 BEARPEX campaign. (a) Average MBO mixing ratio and the MBO organosulfate; (b) Average isoprene mixing ratio and the IEPOX-derived organosulfate. The BVOC mixing ratios are in ppb; the organosulfate mass concentrations are in ng/m^3 .

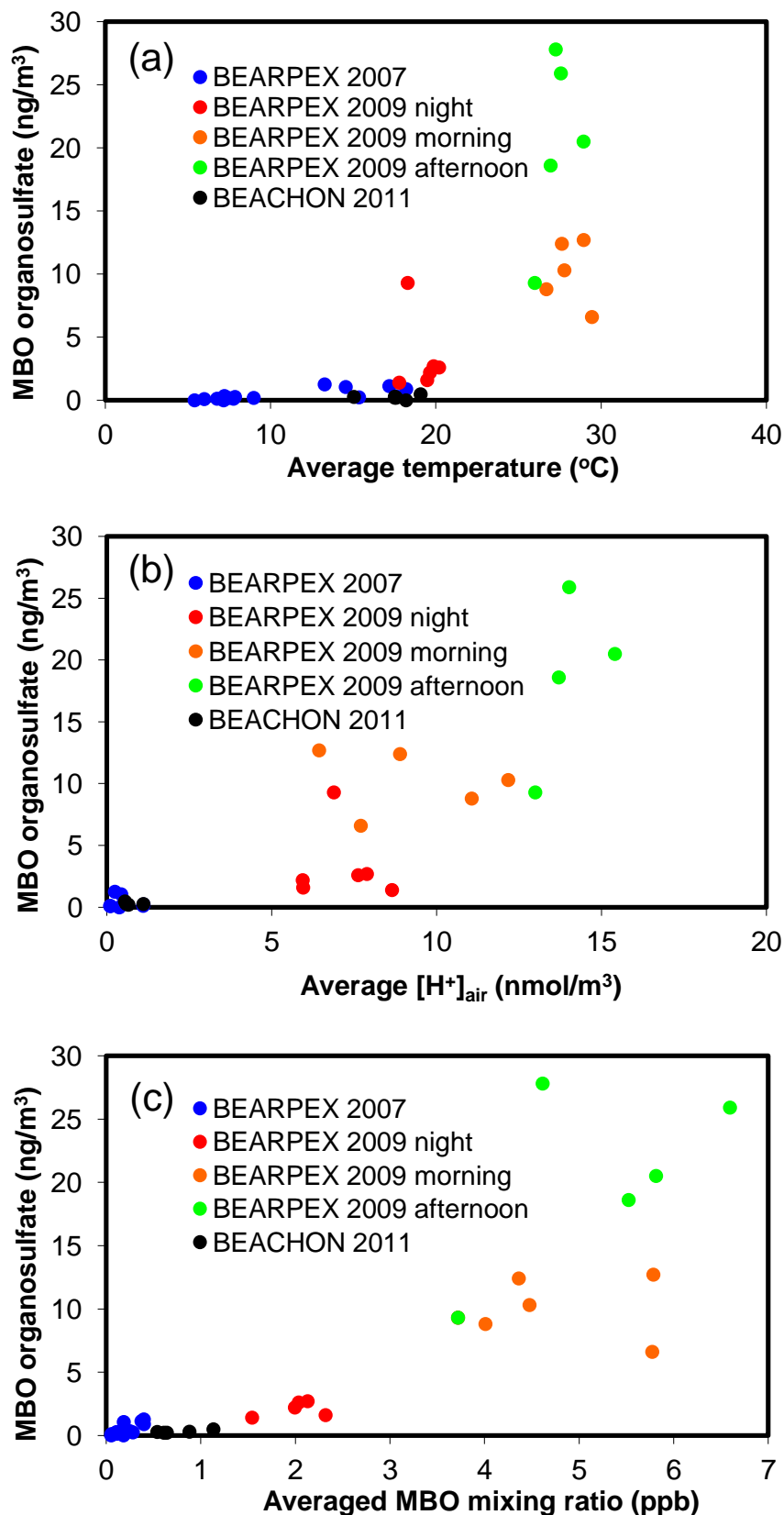
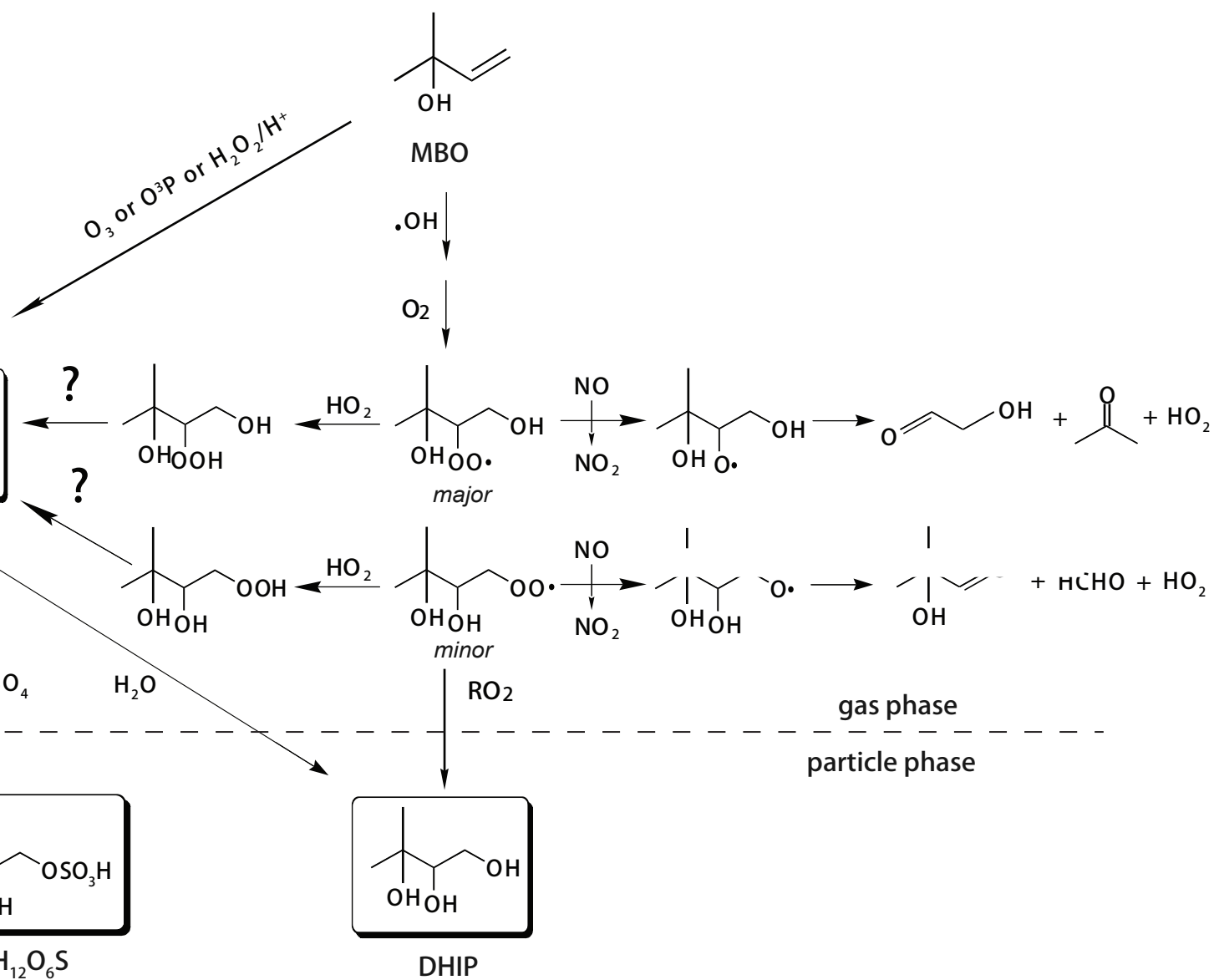


Figure 5. Correlation of the MBO organosulfate mass concentrations to (a) average temperature; (b) average acidity; (c) average MBO mixing ratio from the BEARPEX and BEACHON campaigns. The data from different times of day are shown separately for the BEARPEX 2009 results.

1
2
3
4
5
6
7
8
9
10
11
12
13
14
15
16
17
18
19
20
21
22
23
24
25
26
27
28
29
30
31
32
33
34
35
36
37
38
39
40
41
42
43
44
45
46
47
48
49
50
51
52
53
54
55
56
57
58
59
60



Scheme 1. Proposed mechanism of MBO photooxidation forming SOA. Some structural isomers are not shown.

Supporting Information

Organosulfate Formation from 2-Methyl-3-Buten-2-ol (MBO) as a Secondary Organic Aerosol (SOA) Tracer in the Atmosphere

Haofei Zhang¹, David R. Worton^{2,3}, Michael Lewandowski⁴, John Ortega⁵, Caitlin L. Rubitschun¹, Kasper Kristensen⁶, Pedro Campuzano-Jost^{7,8}, Douglas A. Day^{7,8}, Jose L. Jimenez^{7,8}, Mohammed Jaoui⁹, John H. Offenberg⁴, Tadeusz E. Kleindienst⁴, Jessica Gilman^{7,10}, Joost de Gouw^{7,10}, Changhyoun Park¹¹, Gunnar W. Schade¹¹, Amanda A. Frossard¹², Lynn Russell¹², Lisa Kaser¹³, Werner Jud¹³, Armin Hansel¹³, Luca Cappellin⁵, Thomas Karl⁵, Marianne Glasius⁶, Alex Guenther⁵, Allen H. Goldstein^{2,14}, John H. Seinfeld¹⁵, Avram Gold¹, Richard M. Kamens¹, and Jason D. Surratt^{1,*}

¹Department of Environmental Sciences and Engineering, Gillings School of Global Public Health, The University of North Carolina at Chapel Hill, Chapel Hill, NC, 27599, USA.

²Department of Environmental Science, Policy and Management, University of California, Berkeley, CA, 94720, USA.

³Aerosol Dynamics Inc., Berkeley, CA, 94710, USA.

⁴US Environmental Protection Agency, Office of Research and Development, National Exposure Research Laboratory, Research Triangle Park, NC, 27711, USA.

⁵National Center for Atmospheric Research, Atmospheric Chemistry Division, Boulder, CO, 80301, USA.

⁶Department of Chemistry, Aarhus University, 8000 Aarhus C, Denmark.

⁷Cooperative Institute for Research in Environmental Sciences, University of Colorado, Boulder, CO, 80309, USA.

⁸Department of Chemistry and Biochemistry, University of Colorado, Boulder, CO, 80309, USA.

⁹Alion Science and Technology, P.O. Box 12313, Research Triangle Park, NC, 27709, USA.

¹⁰Chemical Sciences Division, NOAA Earth System Research Laboratory, Boulder, CO, 80305, USA.

¹¹Department of Atmospheric Sciences, Texas A&M University, College Station, TX, 77843, USA.

¹²Scripps Institution of Oceanography, University of California, San Diego, La Jolla, CA, 92093, USA.

¹³Institute of Ion Physics and Applied Physics, University of Innsbruck, Innsbruck, Austria.

¹⁴Department of Civil and Environmental Engineering, University of California, Berkeley, CA, 94720, USA.

¹⁵Department of Chemical Engineering, California Institute of Technology, Pasadena, CA, 91125, USA.

*Corresponding Author: Jason D. Surratt (surratt@unc.edu)

For submission to: Environmental Science & Technology

Table S1. Supporting data from BEARPEX 2007 campaign.

Start Time	average temperature (°C)	average RH (%)	average O ₃ (ppb)	average organics (µg/m ³)	average [H ⁺] ^a (nmol/m ³)	average MBO (ppb)	MBO OS ^b (ng/m ³)	average isoprene (ppb)	IEPOX OS ^b (ng/m ³)	Fraction of MBO OS in total organics
9/20/07 18:45	7.4	89.5	29.8	3.98	0.00	0.10	0.19	0.18	1.63	0.00%
9/21/07 7:45	17.6	42.7	41.2	1.93	0.00	0.25	0.33	0.12	1.87	0.02%
9/21/07 13:15	13.3	62.7	49.8	3.10	0.24	0.40	1.26	0.28	1.23	0.04%
9/21/07 18:45	7.8	82.5	40.9	3.56	NA	0.11	0.27	0.08	0.42	0.01%
9/22/07 7:45	7.2	97.2	NA	2.62	NA	0.18	0.34	NA	1.93	0.01%
9/22/07 13:15	7.2	98.5	34.4	1.46	0.00	0.18	0.00	0.03	0.54	0.00%
9/22/07 18:45	5.4	99.2	29.1	1.53	0.37	0.05	0.00	0.02	0.60	0.00%
9/23/07 7:45	6.8	99.1	37.4	1.24	0.10	0.08	0.13	0.02	0.92	0.01%
9/23/07 13:15	9.0	88.0	34.0	1.71	0.00	0.18	0.19	0.10	1.76	0.01%
9/23/07 18:45	6.0	80.1	27.7	1.38	0.10	0.05	0.10	0.07	1.26	0.01%
9/24/07 7:45	14.5	37.0	37.8	1.39	0.43	0.18	1.05	0.04	1.10	0.08%
9/24/07 13:15	15.3	44.8	48.5	2.92	1.11	0.28	0.24	0.10	1.64	0.01%
9/24/07 18:45	7.7	68.3	41.1	2.46	1.10	0.11	0.13	0.19	2.40	0.01%
9/25/07 7:45	17.2	39.1	NA	NA	NA	0.37	1.13	NA	3.18	NA
9/25/07 13:15	18.2	37.7	NA	3.43	NA	0.40	0.89	NA	3.11	0.03%

^a [H⁺] is calculated from charge balance based on the AMS data of [SO₄²⁻], [NO₃⁻], and [NH₄⁺].

^b "OS" represents organosulfate.

Table S2. Supporting data from BEARPEX 2009 campaign.

Start Time	average temperature (°C)	average RH (%)	average O ₃ (ppb)	average organics (µg/m ³)	average [H ⁺] ^a (nmol/m ³)	average MBO (ppb)	MBO OS ^b (ng/m ³)	average isoprene (ppb)	IEPOX OS ^b (ng/m ³)	Fraction of MBO OS in total organics
7/25/09 19:15	17.8	50.3	45.1	2.42	8.64	1.54	1.39	0.61	6.44	0.06%
7/26/09 8:45	27.8	28.5	49.4	2.26	12.17	4.47	10.31	1.30	8.16	0.46%
7/26/09 14:15	27.6	30.8	64.5	3.04	14.02	6.59	25.86	2.05	10.63	0.85%
7/26/09 19:45	19.6	37.7	51.3	2.16	5.93	1.99	2.18	0.96	8.44	0.10%
7/27/09 8:45	29.4	24.5	54.3	1.95	7.70	5.77	6.59	1.59	9.66	0.34%
7/27/09 14:15	28.9	26.3	70.1	3.18	15.40	5.81	20.55	1.82	10.15	0.65%
7/27/09 19:45	20.2	45.1	50.5	3.08	7.62	2.03	2.60	1.24	11.28	0.08%
7/28/09 8:45	28.9	33.7	53.3	3.36	6.43	5.78	12.69	2.01	10.70	0.38%
7/28/09 14:15	27.2	36.3	68.7	5.19	NA	4.61	27.85	1.22	18.91	0.54%
7/28/09 19:45	19.9	51.9	60.9	4.61	7.88	2.13	2.72	0.67	14.02	0.06%
7/29/09 8:45	27.6	35.3	NA	3.58	8.89	4.36	12.37	1.14	19.40	0.35%
7/29/09 14:15	26.9	41.7	NA	8.37	13.70	5.52	18.56	2.01	17.09	0.22%
7/29/09 19:45	19.5	61.8	NA	5.28	5.95	2.32	1.56	1.51	14.02	0.03%
7/30/09 8:45	26.7	39.8	NA	9.80	11.06	4.01	8.81	1.52	22.57	0.09%
7/30/09 14:15	26.0	42.1	NA	4.63	12.99	3.72	9.26	2.06	25.11	0.20%
7/30/09 19:45	18.3	NA	NA	3.70	6.88	NA	1.83	NA	13.38	0.05%

^a [H⁺] is calculated from charge balance based on the IC measurements of [SO₄²⁻], [NO₃⁻], and [NH₄⁺].

^b “OS” represents organosulfate.

Table S3. Supporting data from BEACHON 2011 campaign.

Start Time ^a	average temperature (°C)	average RH (%)	average O ₃ (ppb)	average organics (µg/m ³)	average [H ⁺] ^b (nmol/m ³)	average MBO (ppb)	MBO OS ^c (ng/m ³)	DHIP ^d (ng/m ³)	IEPOX OS ^c (ng/m ³)	Isoprene tetrols ^e & triols ^f (ng/m ³)	Fraction of MBO OS in total organics
7/23/11 18:40	19.1	48.8	57.6	1.10	0.55	1.13	0.48	0.11	1.61	0.35	0.04%
8/1/11 17:10	15.0	73.5	42.5	1.26	1.10	0.54	0.27	0.08	1.06	0.52	0.02%
8/4/11 18:25	17.6	49.4	43.8	1.16	0.00	0.61	0.21	0.06	1.97	0.48	0.02%
8/7/11 19:45	17.5	39.3	45.9	1.52	0.58	0.88	0.29	0.03	1.05	0.36	0.02%
8/10/11 17:05	17.5	50.2	46.8	1.83	0.65	0.64	0.21	0.02	1.14	0.32	0.01%
8/16/11 18:15	18.2	47.1	39.3	1.30	0.58	0.84	0.00	0.11	0.09	0.48	0.00%

^a The total sampling time for each sample is ~ 3 days (72 hrs); The total sampling volume for each sample is ~ 4320 m³.

^b [H⁺] is calculated from charge balance based on the AMS data of [SO₄²⁻], [NO₃⁻], and [NH₄⁺].

^c “OS” represents organosulfate. Propyl sulfate was used as a surrogate standard for quantification.

^d “DHIP” represents the 2,3-dihydroxyisopentanol measured from GC/EI-MS. *meso*-erythritol was used as a surrogate standard for quantification.

^e “isoprene tetrols” represent the 2-methyltetrols measured from GC/EI-MS. *meso*-erythritol was used as a surrogate standard for quantification.

^f “isoprene triols” represent the C5-alkenetriols measured from GC/EI-MS. *meso*-erythritol was used as a surrogate standard for quantification.

GC/EI-MS chemical analysis to measure DHIP:

Dried residues were trimethylsilylated by the addition of 100 µL of BSTFA + trimethylchlorosilane (99:1 (v/v), Supleco) and 50 µL of pyridine (Sigma-Aldrich, 98%, anhydrous), and the resultant mixture was then heated for 1 h at 70 °C. SOA compounds that contain carboxyl and hydroxyl moieties are converted into volatile trimethylsilyl (TMS) derivatives that can be detected by GC/MS (Surratt et al., 2006). The details of the GC/MS technique and the operation procedures can be found in Zhang et al. (2011).

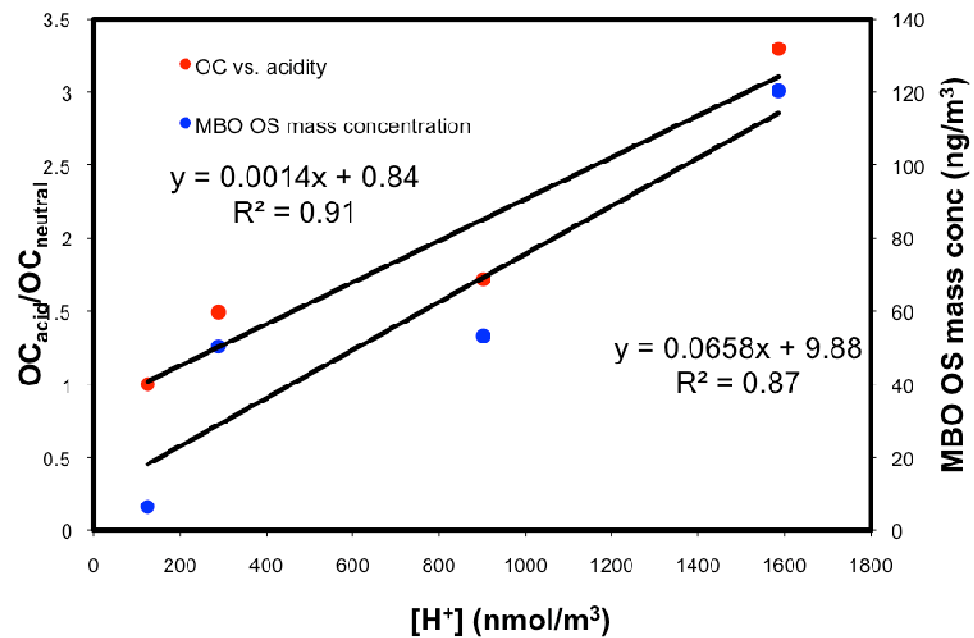


Figure S1. Correlation of the ratio of organic carbon (OC) concentration at elevated acidity relative to the neutral seed case and measured MBO organosulfate to measured aerosol acidity ($[\text{H}^+]_{\text{air}}$ nmol m⁻³).

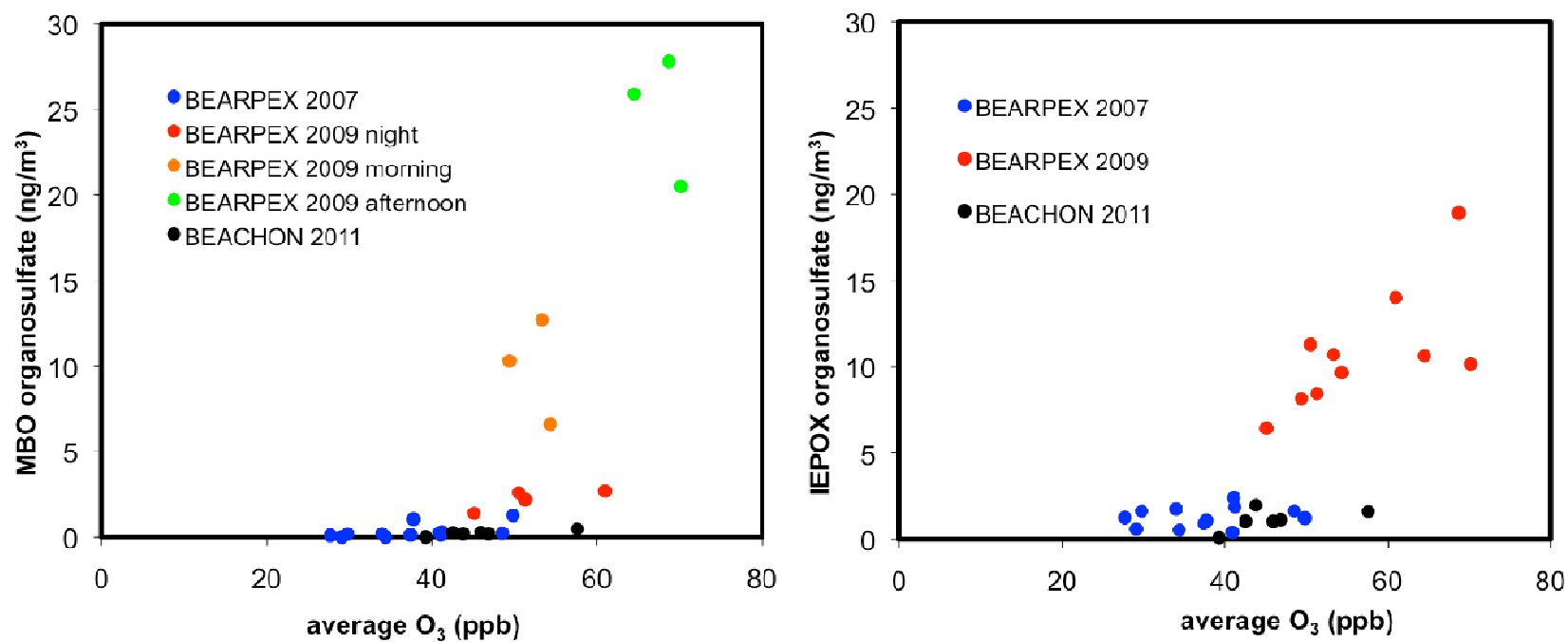


Figure S2. Correlations of MBO organosulfate (a) and IEPOX-derived organosulfate (b) mass concentrations to averaged O₃ from field measurements. The correlations suggest both ozone and organosulfates are secondary pollutants.

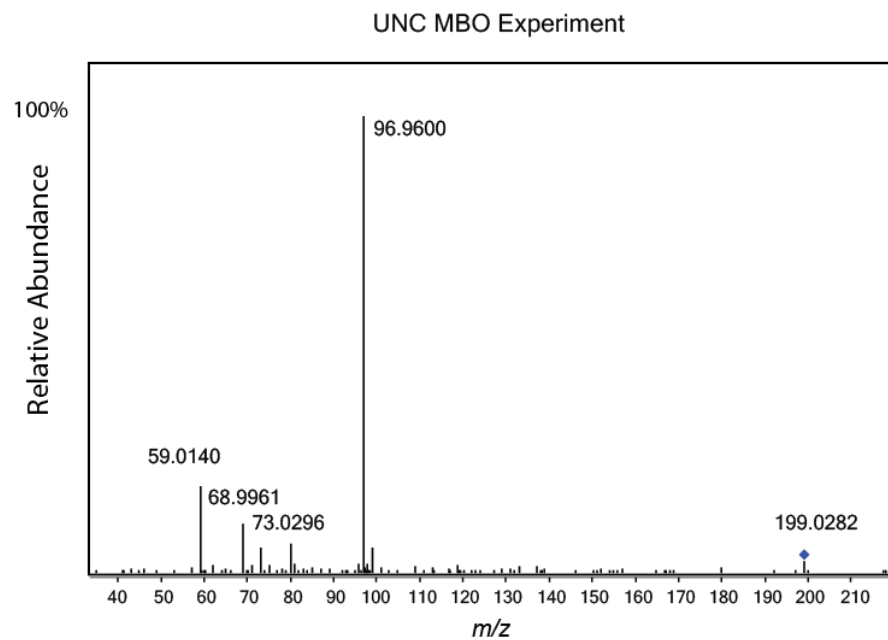


Figure S3. Tandem mass spectra (MS^2) of the MBO organosulfate (m/z 199) measured from the UNC high-NO chamber experiments.

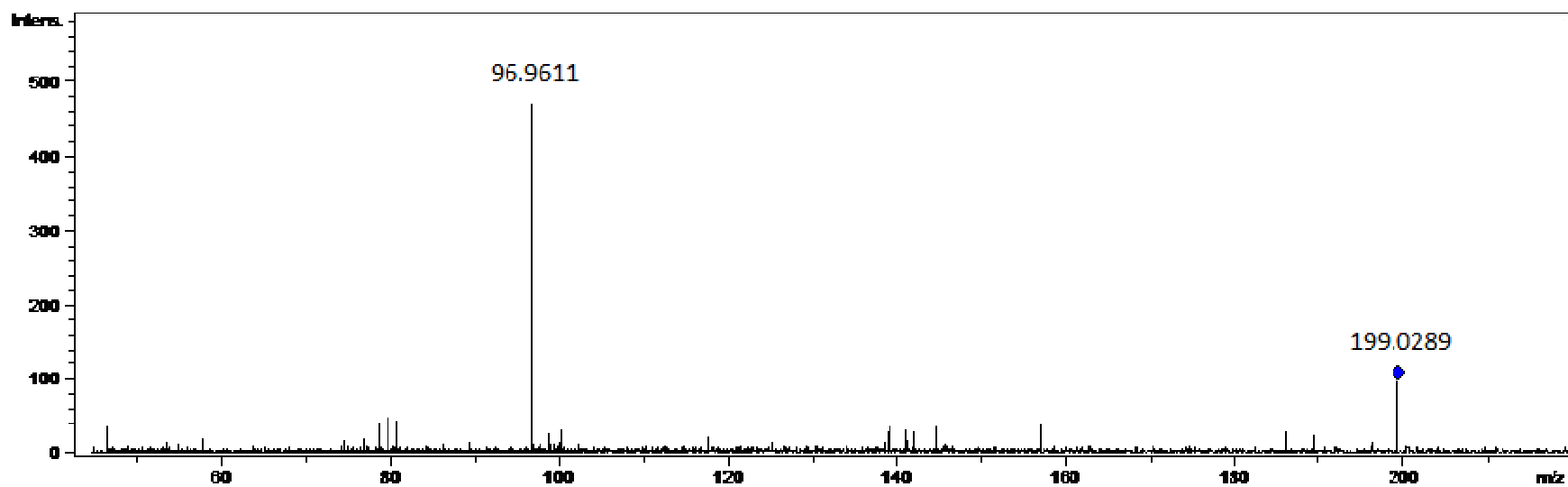


Figure S4. Tandem mass spectra (MS^2) of the MBO organosulfate (m/z 199) measured from the BEARPEX campaigns.

MBO intercalibration at BEARPEX

Measurements of MBO were made at 6.4m (NOAA, 2007) and 17.8m (TAMU, 2009). PTRMS measurements of the sum of MBO plus isoprene were made at five heights (1.5, 6.1, 9.3, 14.3 and 17.8m) through the canopy in both campaigns by the University of California, Berkeley (UCB). The diurnal profiles of MBO and isoprene were very different because MBO is locally emitted and isoprene is advected in from several hours upwind (Figure A). MBO concentrations are dominant over isoprene in the early morning (Figure A) when light and temperature driven emissions accumulate in the shallow boundary layer and transport from upwind is minimal. Figure A shows the comparison of MBO+isoprene (PTRMS) and MBO+isoprene (GC/MS or GC/FID) for the early morning (06:30 – 08:30, 2007; 07:00 – 10:00, 2009) and 2009 (TAMU) when MBO is dominant over isoprene. The comparable slopes of NOAA and TAMU versus UCB show that the MBO calibration scales are similar and that differences in the absolute observed concentrations are due to real variations driven by meteorological conditions between the two campaigns. The MBO+isoprene signal shows a strong vertical gradient through the canopy (Figure B). This gradient is entirely driven by MBO and not isoprene as it is the local emitted species and this is supported by the absence of a gradient in the sum of methyl vinyl ketone and methacrolein (MVK+macr), the first generation oxidation products of isoprene (Figure B). Due to the strong gradient concentrations at 6.1m are 17.8m (Figure B), this difference has not been taken into account in the concentrations reported here but would make the concentrations in 2009 approximately 1.5 times higher.

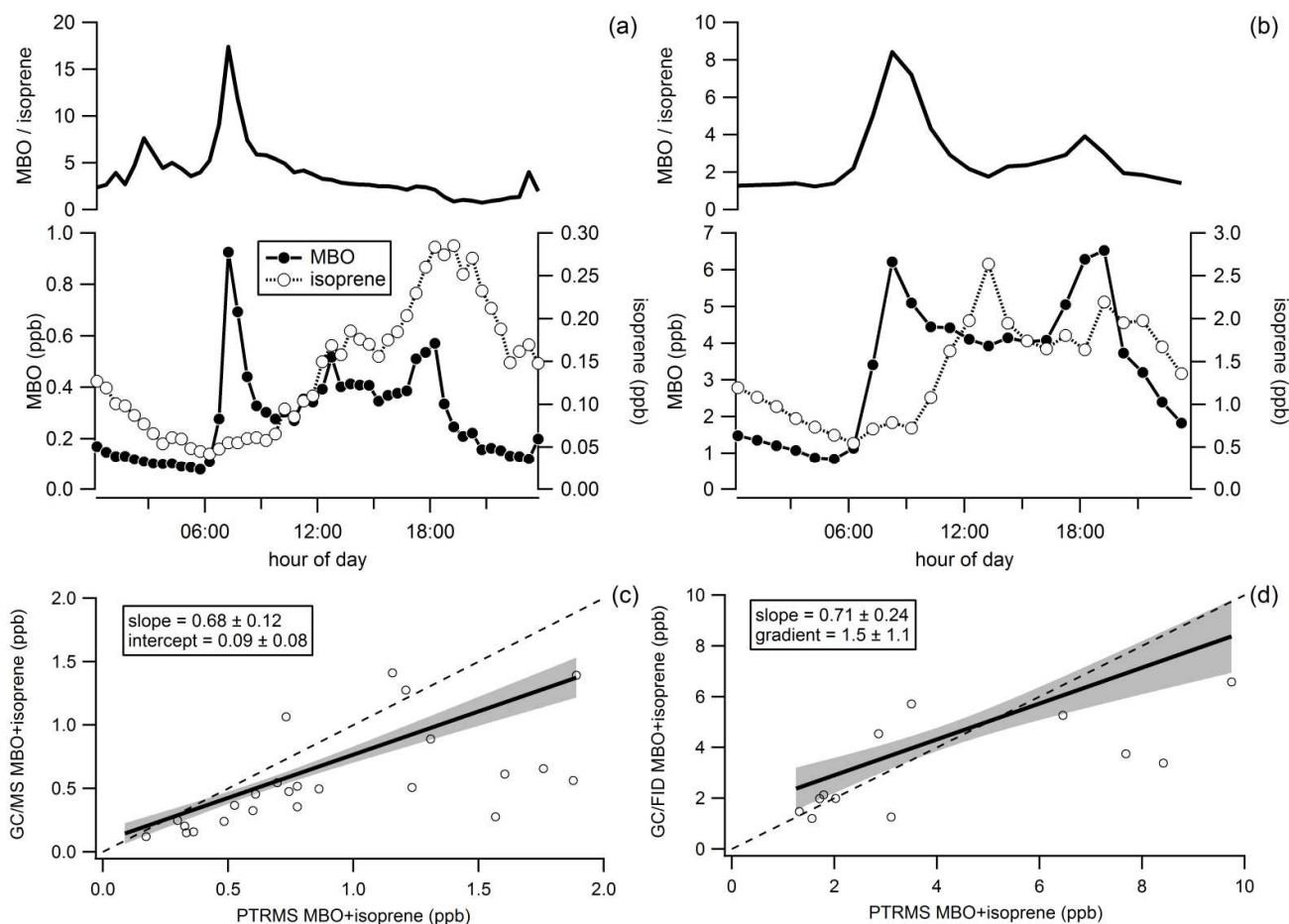


Figure S5. Diurnal variation of MBO, isoprene and the ratio of MBO to isoprene during (a) 2007 and (b) 2009. Comparison of the sum of MBO+isoprene in the early morning only measured by GC and PTRMS during (c) 2007 and (d) 2009.

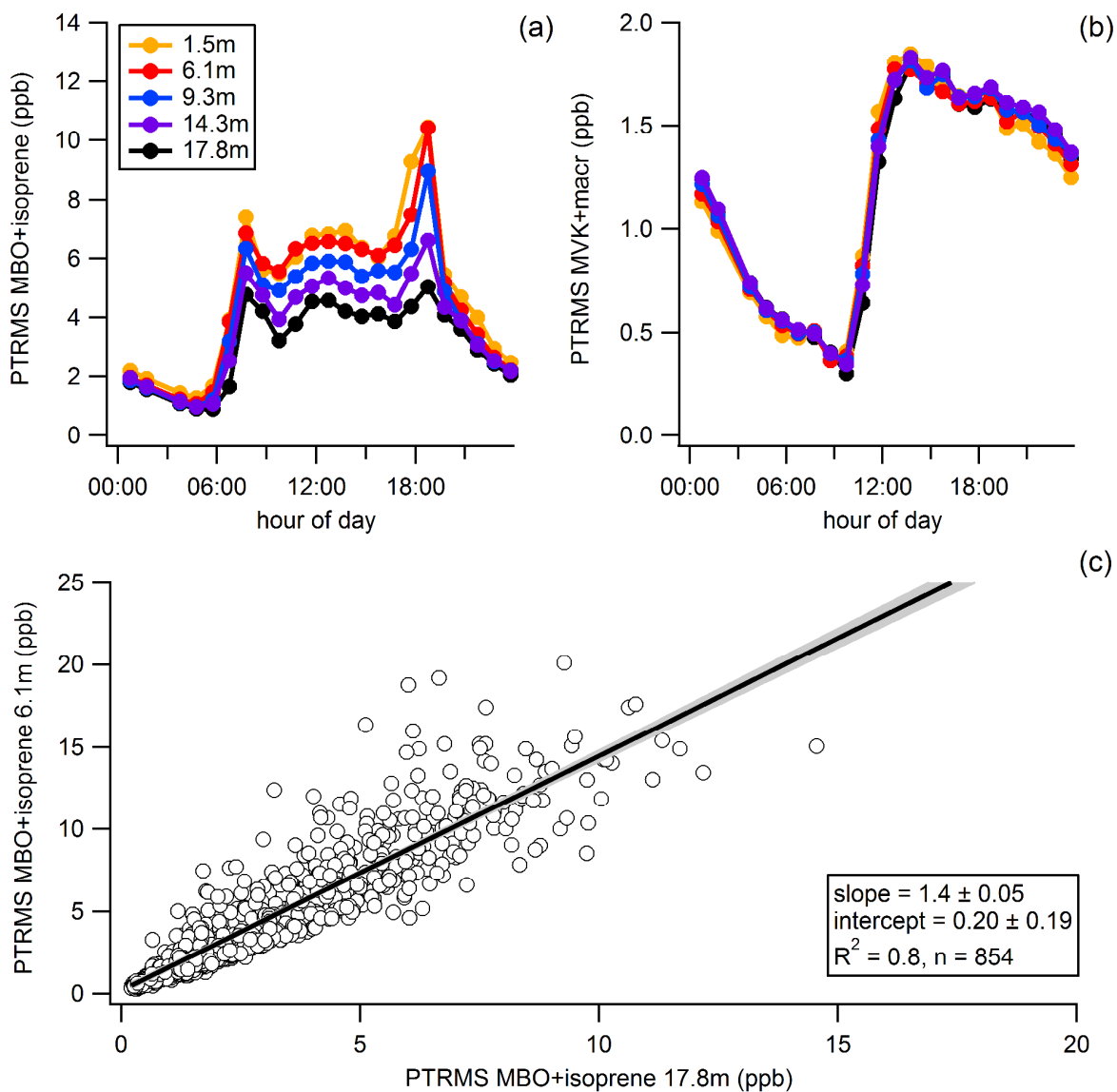


Figure S6. PTRMS gradient measurements at 5 heights (1.5, 6.1, 9.3, 14.3 and 17.8m) in 2009 for (a) MBO+isoprene and (b) methyl vinyl ketone+methacrolien (MVK+macr). Comparison of MBO+isoprene concentrations at 17.8 and 6.1m heights in 2009.